Flatness-based control in successive loops for gas-compressors actuated by IMs and PMSMs

Gerasimos Rigatos[a]
Pierluigi Siano[b]
Bilal Sari[c]

[a]Unit of Industrial Automation
Industrial Systems Institute
26504, Rion Patras Greece
e-mail: grigat@ieee.org

[b]Dept. of Innov. Syst.
University of Salerno
Fisciano, 84084, Italy
e-mail: psiano@unisa.it

[c]Dept. of Electrical Eng.
Université de Setit I
19000, Setif, Algeria
e-mail: bilal.sari@univ-setif.dz

Mohammed AL-Numay[d]
Masoud Abbaszadeh[e]
Gennaro Cuccurullo[f]

[d]Electrical Eng. Dept.
King Saud University
Riyadh 11421, Saudi Arabia
e-mail: alnumay@ksu.edu.sa

[e]Dept. ECS Engineering
Rensselaer Polytech. Inst.
12065, NY, USA
e-mail: masouda@ualberta.ca

[f]Dept. of Industrial Eng.
Univ. of Salerno
Fisciano, 84084, Italy
e-mail: gcuccurullo@unisa.it

Abstract: The article proposes a novel solution to the control problem of centrifugal gas compressors which are driven by three-phase induction motors (IMs) and three-phase permanent magnet synchronous motors (PMSMs), through a novel flatness-based control scheme which is implemented in successive loops. By re-arranging state variables and by splitting suitably the state vector of the IM-driven gas-compressor and of the PMSM-driven gas compressor into subsystems one arrives at writing the associated state-space models in the triangular (strict feedback) form. For the latter state-space description it is possible to solve the control and stabilization problem using chained control loops. The state-space model of the IM-driven gas-compressor and of the PMSM-driven gas-compressor is decomposed into cascading subsystems which satisfy differential flatness properties. For these subsystems virtual control inputs are computed, capable of inverting their dynamics and of eliminating the associated tracking error. The control inputs which are actually applied to the complete nonlinear form of the IM-actuated gas-compressor and of the PMSM-actuated gas compressor are computed from the last subsystem of the chained state-space description. These control inputs incorporate in a recursive manner all virtual control inputs which were computed from the individual subsystems included in the initial state-space equation. The control inputs that should be applied to the nonlinear system so as to assure that all state vector elements will converge to the desirable setpoints are obtained at each iteration of the control algorithm by tracing backwards the subsystems of the chained state-space model. The method is of proven global stability and ensures fast and accurate tracking of the reference setpoints by the state variables of the IM-driven gas compressor and of the PMSM-driven gas compressor.

Keywords: gas compressors, three-phase induction motors, three-phase permanent magnet synchronous motor, multivariable control, differential flatness properties, flatness-based control in successive loops, global stability, Lyapunov analysis.

1 Introduction

Flatness-based control has been one of the main research directions on nonlinear control systems during the last years [1-2]. The method allows for ensuring controllability and designing stabilizing feedback controllers for complex nonlinear dynamical systems [3-5]. A system is considered to be differentially flat if the following two conditions hold: (i) all its state variables and its control inputs can be written as differential functions of a subset of its state variables which define the flat outputs of the system (ii) the flat outputs of the system are differentially independent, which means that they are not connected through a relation in the form of an homogeneous differential equation [6-9]. The proof of differential flatness-properties for a system signifies that through successive differentiations of its flat outputs and a change of state variables the system can be transformed into the input-output linearized form [10-13]. Equivalently differentially flat systems can be written into the canonical Brunovsky form [14-18]. The latter description of the system's state-space model is both controllable and observable and this enables the design of a stabilizing feedback controller with the use of the eigenvalues assignment technique as well as the design of a convergent state estimator, for instance in the form of the Kalman Filter [19-22]. However, to compute the control inputs that should be applied on the initial nonlinear state-space model of the system one should perform inverse transformations, without excluding the appearance of singularities. To avoid such a case and to design a stabilizing feedback controller based on the differential flatness properties of the system, but without the need for changes of state variables, successive differentiations of the flat outputs and state-space model transformations, the present article introduces the concept of flatness-based control in successive loops [23-26].

In the flatness-based control approach in successive loops, the initial nonlinear state-space model of the system is written in the form of a chain of subsystems, where for each one of them it is shown that differential flatness properties hold [23-26]. The state vector of the (i-th) subsystem becomes also a flat outputs vector about it while the state vector of the (i+1)-th subsystem forms a virtual control inputs vector for the i-th subsystem. The proof of differential flatness properties for these subsystems signifies that each one of them can be written in the input-output linearized form and that a stabilizing feedback controller can be designed for each one of them by inverting its dynamics. In this concept, the virtual control inputs vector that stabilizes the (i-th) subsystem should be also a setpoints vector for the (i+1)-th subsystem. Finally, the N-th (last) subsystem in this chain of state-space models contains the real control inputs. The inversion of its dynamics gives the stabilizing feedback controller for the initial nonlinear state-space model. The control signal which achieves stabilization for the initial extended nonlinear state-space model uses recursively the virtual control inputs of the preceding $N-1$ subsystems, by tracing these subsystems backwards that is from the (N-1)-th subsystem to the 1st one. The global stability of the flatness-based control method in successive loops is proven analytically by showing the asymptotic elimination of the tracking error of each one of the subsystems that constitute the integrated system's dynamics. A global stability proof can be also obtained using Lyapunov analysis [27-29].

In the present article, the flatness-based control method in successive loops is tested in two nonlinear industrial systems: (i) centrifugal gas compressors driven by induction motors (ii) centrifugal gas compressors driven by permanent magnet synchronous motors. Gas compressors are of paramount importance for natural gas processing stations and have progressively become the backbone of the gas distribution network [30-32]. They perform liquidisation of natural gas thus facilitating its storage and transport [33-34]. Besides, they enable the transfer of natural gas through pipelines under agreed pressure specifications [35-36]. The growing interest in the optimized functioning of gas distribution networks and gas terminals has motivated much related research during the last years. Recent advancements on optimization techniques for the gas distribution network are given in [37-40]. Recent advancements in the control of gas compressors and pressure levels in the gas network are outlined in [41-43].

Natural gas compressors exhibit multivariable and nonlinear dynamics [44-46]. If inefficiently controlled gas compressors may exhibit surge, which is associated with unsteady mass flow through the compressor and sustained oscillations that may finally damage the compressor's blades [47- 49]. To treat the complicated nonlinear and multi-variable dynamics of gas compressors elaborated nonlinear control algorithms have been proposed [50-52]. Fault tolerance, precision and robustness are prerequisites for the actuation systems of gas compressors. [53-55]. One can distinguish for instance several results on NMPC (nonlinear model predictive control), as well as on MPC which is applied to linearized models of the compressors [56-57]. Besides, one can note results on the use of global linearization-based control and state estimation-based control [58-60]. Additionally one can find results based on linearization around multiple equilibria and subsequent use of LMI techniques [61-62]. Usually the opening or closure of the compressor's inlet, outlet and retrofitting valves function as control inputs [63-65]. Moreover, when the compressor receives actuation from an electric motor, the motor's torque becomes also a control input that determines significantly the stability properties and the optimal function of the compressor [66-68].

Several types of electric motors have been considered as actuators of centrifugal gas-compressors, and these are mainly synchronous three-phase motors, asynchronous (induction) motors and multi-phase motors [69-72]. To stabilize the functioning of the compressor and to make its input and output pressure as well as its mass flow reach the targeted setpoints, elaborated nonlinear control methods have been proposed [73- 75]. The control problem of distributed gas-compressors is primarily found in gas-processing stations where the aim is to mix volumes of gas, arriving through different gas-transmission pipelines under different mass rate and pressure characteristics [76-79]. Different configurations of gas-compressors, being connected serially or in parallel, can result into gas processing units of nonlinear, complicated and high-dimensional state-space models [80- 83]. The development of nonlinear control and optimization methods that can assure the reliable functioning of such gas-processing stations is obviously a non-trivial task [84-86]. Similar are the control problems in the case of electrically-driven air compressors and this is another industrial domain where the article's results potentially can be used [87 -90].

The present article considers models of gas-compressors with electric actuation coming from either three-phase induction (asynchronous) motors or from three-phase permanent magnet synchronous motors. The global stability properties of the flatness-based control method in successive loops is analytically proven and experimentally confirmed through simulation tests. The structure of the article is as follows: In Section 2 the dynamic model of the induction motor-driven gas-compressor is analyzed. In Section 3 a flatness-based controller in successive loops is designed for the gas compressor with actuation from an induction motor. In Section 4 the dynamic model of the PMSM-driven gas compressor is analyzed. The global stability properties of the associated control loop are proven. In Section 5 a flatness-based controller in successive loops is developed for the dynamic model of the gas compressor with actuation from a PM synchronous motor. The global stability properties of the associated control loop are proven. In Section 6 simulation experiments are performed to test the performance of (i) flatness-based control in successive loops for the dynamic model of the induction motor-driven gas compressor, (ii) flatness-based control in successive loops for the dynamic model of the PMSM-driven gas-compressor. Finally, in Section 7 concluding remarks are stated.

2 Dynamic model of the induction motor-driven gas-compressor

2.1 Dynamics of the IM-driven gas compressor

The diagram of the integrated system which includes a gas compressor that is actuated by an Induction Motor is given in Fig. 1. Two tanks are considered of volumes V_i and V_o respectively. These represent the plenum before and after compression. The inlet tank stores uncompressed gas arriving to it through the inlet valve. The outlet tank stores compressed gas arriving to it through the outlet valve. The pressure of the inlet valve is denoted as p_i. The pressure of the outlet valve is denoted as p_o. The mass flow through the compressor is denoted as m. The mass flow is dependant on the tank volumes and gas velocities, as well as on inlet and outlet tank conditions, denoted as a_i and a_o respectively. The compressor's turn speed, which is also the motor's turn speed is denoted as ω. The compressor's torque is denoted as τ_c. The motor's torque is denoted as τ_d and is a control input for the compressor. The moment of inertia of the turning part of the compressor is denoted as J [32], [66-68], [91].

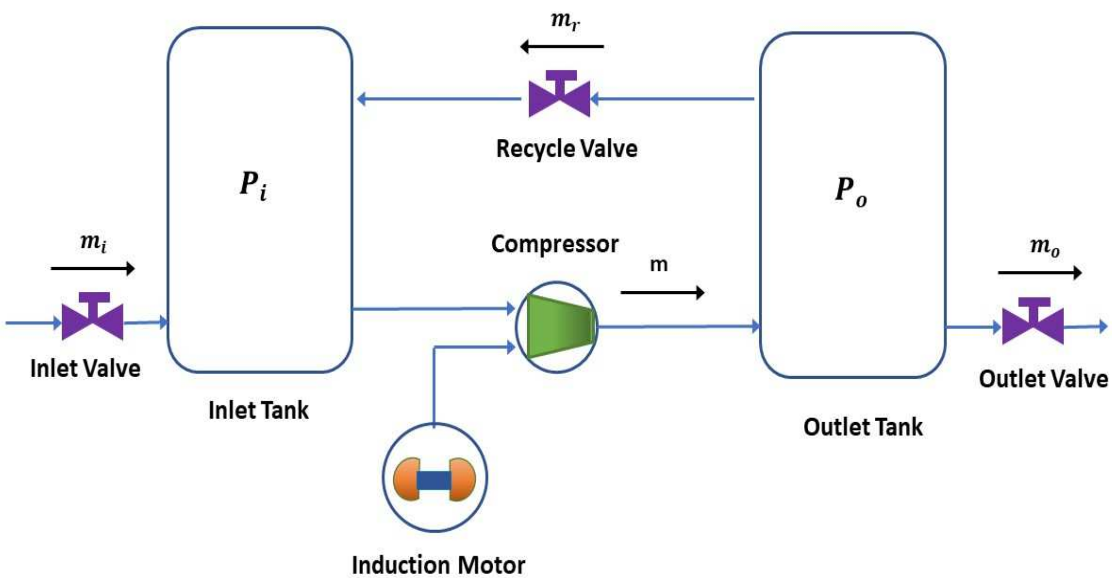

Figure 1: Diagram of the integrated system that includes a gas compressor being actuated by an Induction Motor

The mass flow through the recycle valve is described by a first-order differential equation with a time constant which is denoted as T_r. The steady-state recycle mass flow is denoted as $m_{r,s}$. The compressor's characteristics which define the mass flow rate through it are denoted by function $\pi(m,\omega)$. The compressor's torque τ_c is given by function $\tau_c(m,\omega)$ which signifies that the torque which is developed by the compressor depends on its turn speed and on the mass flow rate through it.In aggregate, the dynamic model of the compressor is given by the following equations [32]:

$$\dot{p}_i = \frac{a_i^2}{V_i}[m_i(p_i) - m + m_p] \tag{1}$$

$$\dot{p}_o = \frac{a_o^2}{V_o}[-m_o(p_o) + m - m_r] \tag{2}$$

$$\dot{m} = \frac{1}{L}[\pi(\omega,m)p_i - p_o] \tag{3}$$

$$\dot{\omega} = \frac{1}{J}[\tau_d - \tau_c(\omega,m) - v\omega] \tag{4}$$

$$\dot{m}_r = \frac{1}{T_r}[m_{r,ss}(p_i, p_o, K_i) - m_i] \tag{5}$$

where v is a mechanical friction coefficient. Besides, about the inlet, outlet and reverse mass flow in the gas compressor it holds that [32]

$$m_i(p_i) = K_i\sqrt{p_{atm} - p_i} \tag{6}$$

$$m_o(p_o) = K_o\sqrt{p_o - p_{atm}} \tag{7}$$

$$m_{r,ss}(p_i, p_o, K_r) = K_r\sqrt{p_2 - p_1} \tag{8}$$

where K_i is the inlet valve constant which is used as a control input, K_o is the outlet valve constant, p_{atm} is the atmospheric pressure and K_r is the recycle valve constant which also serves as a control input. The three valves' constants depend on each valve's throttle position. Non-return values ensure also that mass flow rates m_i, m_o and m_r cannot change direction.

By substituting Eq. (6), Eq. (7) and Eq. (8) into Eq. (1) to Eq. (5) one obtains [32]

$$\dot{p}_i = \frac{a_i^2}{V_i}[K_i\sqrt{p_{atm} - p_i} - m + m_r] \tag{9}$$

$$\dot{p}_o = \frac{a_o^2}{V_o}[-K_o\sqrt{p_o - p_{atm}} + m - m_r] \tag{10}$$

$$\dot{m} = \frac{1}{L}[\pi(\omega, m)p_i - p_o] \tag{11}$$

$$\dot{\omega} = \frac{1}{J}[\tau_d - \tau_c(m, \omega) - v\omega] \tag{12}$$

$$\dot{m}_r = \frac{1}{T_r}[K_r\sqrt{p_o - p_i} - K_i\sqrt{p_{atm} - p_i}] \tag{13}$$

By defining the state vector $x = [x_1, x_2, x_3, x_4, x_5]^T = [p_i, p_o, m, \omega, m_r]^T$ and the control inputs vector K_i, K_r, τ_d the dynamic model of the compressor is written as

$$\dot{x}_1 = \frac{a_i^2}{V_i}[K_i\sqrt{p_{atm} - x_1} - x_3 + x_5] \tag{14}$$

$$\dot{x}_2 = \frac{a_o^2}{V_o}[-K_o\sqrt{x_2 - p_{atm}} + x_3 - x_5] \tag{15}$$

$$\dot{x}_3 = \frac{1}{L}[\pi(x_3, x_4)x_1 - x_2] \tag{16}$$

$$\dot{x}_4 = \frac{1}{J}[\tau_d - \tau_c(x_3, x_4) - vx_4] \tag{17}$$

$$\dot{x}_5 = \frac{1}{T_r}[K_r\sqrt{x_2 - x_1} - K_i\sqrt{p_{atm} - x_1}] \tag{18}$$

Under the assumption of field orientation, the magnetic field of the induction motor rotates asynchronously at a rate which is defined by the first-order time-derivative of the field-orientation angle [3], [1-5]

$$\rho = tan^{-1}(\frac{\psi_{rb}}{\psi_{ra}}) \tag{19}$$

In the dq asynchronously rotating reference frame only the d-axis constituent of the magnetic flux remains while the q-axis constituent of the magnetic flux vanishes, that in $\psi = \psi_{rd}$ and $\psi_{rq} = 0$. In the new coordinates frame the induction motor model is written as: [3], [1-5]

$$\dot{\theta} = \omega \tag{20}$$

$$\dot{\omega} = \frac{\mu}{J}\psi_{rd}i_{sq} - \frac{T_L}{J} - \frac{T_b}{J} \tag{21}$$

$$\dot{\psi}_{rd} = -\alpha\psi_{rd} + \alpha M i_{sd} \tag{22}$$

$$\dot{i}_{sd} = -\gamma i_{sd} + \alpha\beta\psi_{rd} + n_p\omega i_{sq} + \frac{\alpha M {i_{sq}}^2}{\psi_{rd}} + \frac{1}{\sigma L_s}v_{sd} \tag{23}$$

$$\dot{i}_{sq} = -\gamma i_{sq} - \beta n_p\omega\psi_{rd} - n_p\omega i_{sd} - \frac{\alpha M i_{sq}i_{sd}}{\psi_d} + \frac{1}{\sigma L_s}v_{sq} \tag{24}$$

$$\dot{\rho} = n_p\omega + \frac{\alpha M i_{sq}}{\psi_{rd}} \tag{25}$$

In Eq. (21) T_L is the load torque and in the case of the compressor $T_L = \tau_c(m,\omega)$, while T_b is the torque due to mechanical friction with $T_b = v\omega$. M denotes mutual inductance, and n_p is the number of poles. Parameters σ, γ, μ, a and β are associated with the coefficients of the electric circuit of the stator and the rotor (resistance, inductance, mutual inductance and number of poles) [1-5], [91]. Next, the following state variables are defined: $x = [x_6, x_7, x_8, x_9]^T = [\psi_{rd}, i_{sd}, i_{sq}, \rho]^T$ while the control inputs vector is $u = [v_{sd}, v_{sq}]^T$. Thus, in the dynamic model of the induction motor the driving torque is rewritten as

$$\tau_d = \mu x_6 x_8 \tag{26}$$

while about the dynamics of the electric part of the induction motor one has

$$\dot{x}_6 = -\alpha x_6 + \alpha M x_7 \tag{27}$$

$$\dot{x}_7 = -\gamma x_7 + \alpha\beta x_6 + n_p x_4 x_8 + \frac{\alpha M x_8^2}{x_6} + \frac{1}{\sigma L_s}v_{sd} \tag{28}$$

$$\dot{x}_8 = -\gamma x_8 - \beta n_p x_4 x_6 - n_p x_4 x_7 - \frac{\alpha M x_8 x_7}{x_6} + \frac{1}{\sigma L_s}v_{sq} \tag{29}$$

$$\dot{x}_9 = n_p x_4 + \frac{\alpha M x_8}{x_6} \tag{30}$$

2.2 State-space model of the electrically actuated gas compressor

The state vector of the integrated gas compression system which consists of a centrifugal gas-compressor and a three-phase induction motor is given by:

$$\begin{gathered} x = [x_1, x_2, x_3, x_4, x_5, x_6, x_7, x_8, x_9]^T \Rightarrow \\ x = [P_i, P_o, m, \omega, m_r, \psi_{r_d}, i_{s_d}, i_{s_q}, \rho]^T \end{gathered} \tag{31}$$

The dynamic model of the induction motor-driven has the following state-space description

$$
\begin{pmatrix} \dot{x}_1 \\ \dot{x}_2 \\ \dot{x}_3 \\ \dot{x}_4 \\ \dot{x}_5 \\ \dot{x}_6 \\ \dot{x}_7 \\ \dot{x}_8 \\ \dot{x}_9 \end{pmatrix} = \begin{pmatrix} \frac{a_i^2}{V_i}(-x_3+x_5) \\ \frac{a_o^2}{V_o}[-K_o\sqrt{x_2-p_{atm}}+x_3-x_5] \\ \frac{1}{L}[\pi(x_3,x_4)x_1-x_2] \\ \frac{1}{J}[\mu x_6 x_8-\tau_c(x_3,x_4)-v x_4] \\ 0 \\ -a x_6+aMx_7 \\ -\gamma x_7+a\beta x_6+n_p x_4 x_6+\frac{aMx_8^2}{x_6} \\ -\gamma x_6-\beta n_p x_4 x_6-n_p x_4 x_7-\frac{aMx_8 x_7}{x_6} \\ n_p x_4+\frac{aMx_8}{x_6} \end{pmatrix} + \begin{pmatrix} \frac{a_i^2}{V_i}\sqrt{p_{atm}-x_1} & 0 & 0 & 0 \\ 0 & 0 & 0 & 0 \\ 0 & 0 & 0 & 0 \\ 0 & 0 & 0 & 0 \\ 0 & 0 & 0 & 0 \\ -\frac{1}{T_r}\sqrt{p_{atm}-x_1} & \frac{1}{T_r}\sqrt{x_2-x_1} & 0 & 0 \\ 0 & 0 & 0 & 0 \\ 0 & 0 & \frac{1}{\sigma L_s} & 0 \\ 0 & 0 & 0 & \frac{1}{\sigma L_s} \\ 0 & 0 & 0 & 0 \end{pmatrix} \begin{pmatrix} u_1 \\ u_2 \\ u_3 \\ u_4 \end{pmatrix} \tag{32}
$$

First, the rows of the state-space model are reorganized as follows:

$$\dot{x}_2 = \frac{a_o^2}{V_o}[-K_o\sqrt{x_2-p_{atm}}+x_3-x_5] \tag{33}$$

$$\dot{x}_3 = \frac{1}{L}[\pi(x_3,x_4)x_1-x_2] \tag{34}$$

$$\dot{x}_4 = \frac{1}{J}[\mu x_6 x_8-\tau_c(x_3,x_4)-v x_4] \tag{35}$$

$$\dot{x}_6 = -a x_6+aMx_7 \tag{36}$$

$$\dot{x}_1 = \frac{a_i^2}{V_i}(-x_3+x_5)+\frac{a_i^2}{V_i}\sqrt{p_{atm}-x_1}u_1 \tag{37}$$

$$\dot{x}_5 = -\frac{1}{T_r}\sqrt{p_{atm}-x_1}u_1+\frac{1}{T_r}\sqrt{x_2-x_1}u_2 \tag{38}$$

$$\dot{x}_7 = -\gamma x_7+a\beta x_6+n_p x_4 x_6+\frac{aMx_8^2}{x_6}+\frac{1}{\sigma L_s}u_3 \tag{39}$$

$$\dot{x}_8 = -\gamma x_6-\beta n_p x_4 x_6-n_p x_4 x_7-\frac{aMx_8 x_7}{x_6}+\frac{1}{\sigma L_s}u_4 \tag{40}$$

The integrated system can be also written in the concise nonlinear affine-in-the-input state-space form

$$\dot{x} = f(x)+g(x)u \tag{41}$$

where $x \in R^{9\times 1}$, $f(x) \in R^{9\times 1}$, $g(x) \in R^{9\times 4}$ and $u \in R^{4\times 1}$.

Next, the state variable of the electrically actuated system are re-defined as follows: $z_1 = x_2$, $z_2 = x_3$, $z_3 = x_4$, $z_4 = x_6$, $z_5 = x_1$, $z_6 = x_5$, $z_7 = x_7$ and $z_8 = x_8$. By substituting state variables x_i by state variables z_i one obtains

$$\dot{z}_1 = \frac{a_o^2}{V_o}[-K_o\sqrt{z_1-p_{atm}}+z_2-z_6] \tag{42}$$

$$\dot{z}_2 = \frac{1}{L}[\pi(z_2,z_3)z_5-z_1] \tag{43}$$

$$\dot{z}_3 = \frac{1}{J}[\mu z_4 z_8-\tau_c(z_2,z_3)-v z_3] \tag{44}$$

$$\dot{z}_4 = -a z_4+aMz_7 \tag{45}$$

$$\dot{z}_5 = \tfrac{a_i^2}{V_i}(-z_2 + z_6) + \tfrac{a_i^2}{V_i}\sqrt{p_{atm} - z_5}u_1 \tag{46}$$

$$\dot{z}_6 = -\tfrac{1}{T_r}\sqrt{p_{atm} - z_5}u_1 + \tfrac{1}{T_r}\sqrt{z_1 - z_5}u_2 \tag{47}$$

$$\dot{z}_7 = -\gamma z_7 + a\beta z_4 + n_p z_3 z_4 + \tfrac{aMz_2^2}{z_4} + \tfrac{1}{\sigma L_s}u_3 \tag{48}$$

$$\dot{z}_8 = -\gamma z_4 - \beta n_p z_3 z_4 - n_p z_3 z_7 - \tfrac{aMz_8 z_7}{z_4} + \tfrac{1}{\sigma L_s}u_4 \tag{49}$$

Thus, the state-space model of the induction motor-driven gas compressor takes the following form:

$$\begin{pmatrix} \dot{z}_1 \\ \dot{z}_2 \\ \dot{z}_3 \\ \dot{z}_4 \\ \dot{z}_5 \\ \dot{z}_6 \\ \dot{z}_7 \\ \dot{z}_8 \end{pmatrix} = \begin{pmatrix} \frac{a_o^2}{V_o}[-K_o\sqrt{z_1 - p_{atm}} + z_2 - z_6] \\ \frac{1}{L}[\pi(z_2, z_3)z_5 - z_1] \\ \frac{1}{J}[\mu z_4 z_8 - \tau_c(z_2, z_3) - vz_3] \\ -az_4 + aMz_7 \\ \frac{a_i^2}{V_i}(-z_2 + z_6) \\ 0 \\ -\gamma z_7 + a\beta z_4 + n_p z_3 z_4 + \frac{aMz_2^2}{z_4} \\ -\gamma z_4 - \beta n_p z_3 z_4 - n_p z_3 z_7 - \frac{aMz_8 z_7}{z_4} \end{pmatrix} + \begin{pmatrix} 0 & 0 & 0 & 0 \\ 0 & 0 & 0 & 0 \\ 0 & 0 & 0 & 0 \\ 0 & 0 & 0 & 0 \\ \frac{a_i^2}{V_i}\sqrt{p_{atm} - z_5} & 0 & 0 & 0 \\ -\frac{1}{T_r}\sqrt{p_{atm} - z_5} & \frac{1}{T_r}\sqrt{z_1 - z_5} & 0 & 0 \\ 0 & 0 & \frac{1}{\sigma L_s} & 0 \\ 0 & 0 & 0 & \frac{1}{\sigma L_s} \end{pmatrix} \begin{pmatrix} u_1 \\ u_2 \\ u_3 \\ u_4 \end{pmatrix} \tag{50}$$

Next, subsystem Σ_1 is defined with the following subvectors and submatrices: $z_{1,4} = [z_1, z_2, z_3, z_4]^T$, $f_{1,4}(z_{1,4})$ and $g_{1,4}(z_{1,4})$

$$f_{1,4} = \begin{pmatrix} \frac{a_o^2}{V_o}[-K_o\sqrt{z_1 - p_{atm}} + z_2] \\ -\frac{1}{L}z_1 \\ \frac{1}{J}[-\tau_c(z_2, z_3) - vz_3] \\ -az_4 + aMz_7 \end{pmatrix} \quad g_{1,4} = \begin{pmatrix} 0 & -\frac{a_o^2}{V_o} & 0 & 0 \\ \frac{1}{L}[\pi(z_2, z_3) & 0 & 0 & 0 \\ 0 & 0 & 0 & \frac{1}{J}[\mu z_4 \\ 0 & 0 & aM & 0 \end{pmatrix} \tag{51}$$

Moreover, subsystem Σ_2 is defined with the following subvectors and submatrices: $z_{5,8} = [z_5, z_6, z_7, z_7]^T$, $f_{5,8}(z_{1,4}, z_{5,8})$ and $g_{5,8}(z_{1,4}, z_{5,8})$

$$f_{5,8} = \begin{pmatrix} \frac{a_i^2}{V_i}(-z_2 + z_6) \\ 0 \\ -\gamma z_7 + a\beta z_4 + n_p z_3 z_4 + \frac{aMz_2^2}{z_4} \\ -\gamma z_4 - \beta n_p z_3 z_4 - n_p z_3 z_7 - \frac{aMz_8 z_7}{z_4} \end{pmatrix} \quad g_{5,8} = \begin{pmatrix} \frac{a_i^2}{V_i}\sqrt{p_{atm} - z_5} & 0 & 0 & 0 \\ -\frac{1}{T_r}\sqrt{p_{atm} - z_5} & \frac{1}{T_r}\sqrt{z_1 - z_5} & 0 & 0 \\ 0 & 0 & \frac{1}{\sigma L_s} & 0 \\ 0 & 0 & 0 & \frac{1}{\sigma L_s} \end{pmatrix} \tag{52}$$

Thus, the dynamic model of the induction motor-driven gas-compressor can be now written in the form of the two chained subsystems Σ_1 and Σ_2

$$\dot{z}_{1,4} = f_{1,4(z_{1,4})} + g_{1,4}(z_{1,4})z_{5,8} \tag{53}$$

$$\dot{z}_{5,8} = f_{5,8}(z_{1,4}, z_{5,8}) + g_{5,8}(z_{1,4})z_{5,8}u \tag{54}$$

2.3 Differential flatness of the IM-driven gas compressor

It can be proven that the state-space model of the IM-driven gas compressor which consists of the cascading subsystems of Eq. (53) and Eq. (54) is differentially flat, with flat outputs vector $y_1 = z_{1,4}$. From Eq.(53) one solves for subvector $z_{5,8}$ which gives

$$z_{5,8} = g_{1,4}(z_{1,4})^{-1}[\dot{z}_{1,4} - f_{1,4}(z_{1,4})] \Rightarrow z_{5,8} = h_a(z_{1,4}, \dot{z}_{1,4}) \tag{55}$$

which signifies that $z_{5,8}$ is a differential function of the flat outputs vector of the system. Moreover, from Eq. (54) one solves for the control input u. This gives

$$u = g_{5,8}(z_{1,4}, z_{5,8})^{-1}[\dot{z}_{5,8} - f_{5,8}(z_{1,4}, z_{5,8})] \Rightarrow u = h_b(z_{1,4}, \dot{z}_{1,4}) \tag{56}$$

which signifies that u is a differential function of the flat outputs vector of the system. This comes to confirm that the integrated gas-compression system is differentially flat.

3 Flatness-based controller in successive loops for the IM-driven gas-compressor

It will be proven that each one of the subsystems Σ_1 and Σ_2 of Eq. (53) and Eq. (54) which constitute the dynamics of the induction motor-driven gas compressor is a differentially flat subsystem. Indeed in the subsystem of Eq. (53) the flat output is taken to be $y_1 = z_{1,4}$ and the virtual control input is $v_1 = z_{5,8}$. Then, solving Eq. (53) for the virtual control input v_1 one has

$$v_1 = g_{1,4}(z_{1,4})^{-1}[\dot{z}_{1,4} - f_{1,4}(z_{1,4})] \tag{57}$$

which signifies that v_1 is a differential function of the flat output y_1. Consequently, Eq. (53) represents a differentially flat subsystem. Next, in the subsystem of Eq. (54) the flat output is taken to be $y_2 = z_{5,8}$, and $z_{1,4}$ is considered to be a coefficients vector and u is the real control input. Solving for u gives

$$u = g_{5,8}(z_{1,4}, z_{5,8})^{-1}[\dot{z}_{1,4} - f_{5,8}(z_{1,4}, z_{5,8})] \tag{58}$$

Consequently, u is a differential function of the flat output y_2 and the subsystem of Eq. (54) is also differentially flat.

Knowing that the subsystems of Eq. (53) and Eq. (54) are differentially flat, it is also inferred that they can be written in the input-output linearized form. Next, a stabilizing feedback controller can be designed for each one of them by inverting their dynamics, as it is commonly done for input-output linearized systems.

For the subsystem of Eq. (53), the stabilizing feedback control input which is provided by $v_1 = z_{5,8}$ is

$$v_1 = g_{1,4}(z_{1,4})^{-1}[\dot{z}_{1,4}^d - f_{1,4}(z_{1,4}) - K_1(z_{1,4} - z_{1,4}^d))] \tag{59}$$

Next, the value of the virtual control input $v_1 = z_{5,8}^d$ becomes setpoint $z_{5,8}^d$ for the subsystem of Eq. (54). The stabilizing feedback control for the latter subsystem, coming from the real control input u is given by

$$u = g_{5,8}(z_{1,4}, z_{5.8})^{-1}[\dot{z}_{5,8}^d - f_{5,8}(z_{1,4}, z_{5.8}) - K_2(z_{5,8} - z_{5,8}^d))] \tag{60}$$

By substituting Eq. (59) into Eq. (53) and by defining the tracking error variable $e_{1,4} = z_{1,4} - z_{1,4}^d$, as well as the diagonal gain matrix $K_1 \in R^{4\times 4} > 0$ with diagonal elements $k_{1,ii} > 0$ for $i = 1, \cdots, 4$, one obtains the tracking error dynamics for the first subsystem. This is given by:

$$\begin{array}{c} \dot{z}_{1,4} = f_{1,4}(z_{1,4}) + g_{1,4}(z_{1,4})g_{1,4}(z_{1,4})^{-1}[\dot{z}_{1,4}^d - f_{1,4}(z_{1,4}) - K_1(z_{1,4} - z_{1,4}^d)] \Rightarrow \\ (\dot{z}_{1,4} - \dot{z}_{1,4}^d) + K_1(z_{1,4} - z_{1,4}^d) = 0 \Rightarrow \dot{e}_{1,4} + K_1 e_{1,4} = 0 \Rightarrow \\ \lim_{t\to\infty} e_{1,4}(t) = 0 \Rightarrow z_{1,4} = z_{1,4}^d \end{array} \tag{61}$$

By substituting Eq. (60) into Eq. (54) and by defining the tracking error8 variable $e_{5,8} = z_{5,8} - z_{5,8}^d$, as well as the diagonal gain matrix $K_2 \in R^{4\times 4} > 0$ with diagonal elements $k_{2,ii} > 0$ for $i = 1, \cdots, 4$, one obtains the tracking error dynamics for the first subsystem. This is given by:

$$\begin{array}{c} \dot{z}_{5,8} = f_{5,8}(z_{1,4}, z_{5,8}) + g_{5,8}(z_{1,4}, z_{5,8}) g_{5,8}(z_{1,4}, z_{5,8})^{-1}[\dot{z}_{5,8}^d - f_{5,8}(z_{1,4}, z_{5,8}) - K_2(z_{5,8} - z_{5,8}^d)] \Rightarrow \\ (\dot{z}_{5,8} - \dot{z}_{5,8}^d) + K_2(z_{5,8} - z_{5,8}^d) = 0 \Rightarrow \dot{e}_{5,8} + K_2 e_{5,8} = 0 \Rightarrow \\ \lim_{t\to\infty} e_{5,8}(t) = 0 \Rightarrow z_{5,8} = z_{5,8}^d \end{array} \tag{62}$$

Consequently, all state vector elements z_i $i = 1. \cdots, 8$ converge to the associated setpoints z_i^d and through them the state variables of the initial nonlinear system x_i, $i = 1, \cdots, 8$ converge to the associated setpoints x_i^d. Therefore, the control loop of the induction motor-driven gas-compressor is globally asymptotically stable.

Global stability for the control loop of the IM-driven gas compressor can be also proven through Lyapunov analysis. To this end, the following Lyapunov function is defined

$$V = \frac{1}{2}[e_{1,4}^T e_{1,4} + e_{5,8}^T e_{5,8}] \tag{63}$$

By differentiating in time one obtains

$$\dot{V} = \frac{1}{2} 2[e_{1,4}^T \dot{e}_{1,4} + e_{5,8}^T \dot{e}_{5,8}] \tag{64}$$

Next, using the relations about the tracking error dynamics of the system's subvectors which was given in E q. 61 and Eq. (62) one obtains

$$\begin{array}{c} \dot{V} = [e_{1,4}^T(-K_1 e_{1,4}) + e_{5,8}^T(-K_2 e_{5,8})] \Rightarrow \\ \dot{V} = -[e_{1,4}^T K_1 e_{1,4} - e_{5,8}^T K_2 e_{5,8}] \Rightarrow \\ \dot{V} < 0 \ \forall \ e_{1,4} \neq 0, \ e_{5,8} \neq 0 \end{array} \tag{65}$$

Moreover, $\dot{V} = 0$ if and only if $e_{1,4} = 0$ and $e_{5,8} = 0$. consequently V is a strictly diminishing function which converges asymptotically to the equilibrium $[e_{1,4} = 0, \ e_{5,8} = 0]$. Thus, once again global asymptotic stability is proven for the control loop of the induction motor-driven gas-compressor.

4 Dynamic model of the PMSM-driven gas-compressor

4.1 Dynamics of the PMSM-driven gas compressor

The diagram of the PMSM electrically-driven gas compression system is given in Fig. 2/ The pressure of the inlet valve is denoted again as P_i. The pressure of the outlet valve is denoted as P_o. The mass flow through the compressor is denoted as m. The mass flow depends on the tank volumes and gas velocities, as well as on inlet and outlet tank conditions. The compressor's turn speed is denoted as ω. The compressor's torque is denoted as τ_c. The motor's torque is denoted as τ_d and is a control input for the compressor. The moment of inertia of the turning part of the compressor is denoted as J. By defining the state vector of the electrically driven gas compressor as $x_a = [x_1, x_2, x_3, x_4, x_5]^T = [P_i, P_o, m, \omega, m_r]^T$ the associated state-space model is given by [32], [91]

$$\begin{array}{c} \dot{x}_1 = \frac{a_i^2}{V_i}[K_i\sqrt{p_{atm} - x_1} - x_3 + x_5] \\ \dot{x}_2 = \frac{a_o^2}{V_o}[-K_o\sqrt{x_2 - p_{atm}} + x_3 - x_5] \\ \dot{x}_3 = \frac{1}{L}[\pi(x_3, x_4)x_1 - x_2] \\ \dot{x}_4 = \frac{1}{J}[\tau_d - \tau_c(x_3, x_4) - v x_4] \\ \dot{x}_5 = \frac{1}{T_r}[K_r\sqrt{x_2 - x_1} - K_i\sqrt{p_{atm} - x_1}] \end{array} \tag{66}$$

By defining the state vector of the permanent magnet synchronous motor as $x_b = [x_6, x_7, x_8, x_9]^T = [\theta, \omega, i_d, i_q]^T$ the state-space model of this electric motor is given by [3-5]

$$\begin{array}{c} \dot{x}_6 = x_7 \\ \dot{x}_7 = \frac{1}{J}[px_9(\Psi_m - (L_d - L_q)x_8) - Bx_7 - T_L] \\ \dot{x}_8 = \frac{1}{L_d}(v_d - Rx_8 - px_7 L_q x_9) \\ \dot{x}_9 = \frac{1}{L_q}(v_q - Rx_9 - px_7 L_d x_8 - x_7 \Psi_m) \end{array} \tag{67}$$

where J is the moment of inertia of the PMSM, p is the number of poles, Ψ_m is the magnetic flux due to the machine's permanent magnets, L_d, L_q are the inductance coefficients in the dq reference frame, R is the stator's resistance and B is the mechanical friction coefficient.

Using that the torque which provides the rotational motion of the compressor is the electromagnetic torque of the PMSM, that is

$$\tau_d = px_9(\Psi_m - (L_d - L_q)x_8) \tag{68}$$

and applying Eq. (66) about the dynamics of the compressor, as well as Eq. (67) about the dynamics of the PMSM, and by considering that the complete state vector of the integrated system is

$$x = [x_1, x_2, x_3, x_4, x_5, x_6, x_7]^T = [P_i, P_o, m, \omega, m_r, i_d, i_q]^T \tag{69}$$

and that the control inputs vector of the integrated system is

$$u = [u_1, u_2, u_3, u_4]^T = [K_i, K_r, v_d, v_q]^T \tag{70}$$

the integrated state-space model of the compressor-PMSM system comprises the following equations

$$\dot{x}_1 = \frac{a_i^2}{V_i}[u_1\sqrt{p_{atm} - x_1} - x_3 + x_5] \tag{71}$$

$$\dot{x}_2 = \frac{a_o^2}{V_o}[-K_o\sqrt{x_2 - p_{atm}} + x_3 - x_5] \tag{72}$$

$$\dot{x}_3 = \frac{1}{L}[\pi(x_3, x_4)x_1 - x_2] \tag{73}$$

$$\dot{x}_4 = \frac{1}{J}\{[px_7(\Psi_m - (L_d - L_q)x_6)] - \tau_c(x_3, x_4) - vx_4\} \tag{74}$$

$$\dot{x}_5 = \frac{1}{T_r}[u_2\sqrt{x_2 - x_1} - u_1\sqrt{p_{atm} - x_1}] \tag{75}$$

$$\dot{x}_6 = \frac{1}{L_d}(u_3 - Rx_6 - px_4 L_q x_7) \tag{76}$$

$$\dot{x}_7 = \frac{1}{L_q}(u_4 - Rx_7 - px_4 L_d x_6 - x_4 \Psi_m) \tag{77}$$

The previous state-space model of Eq. (71) to Eq. (77) can be also written in the nonlinear affine-in-the-input state-space form

$$\dot{x} = f(x) + g(x)u \tag{78}$$

where $x \in R^{7\times 1}$, $f(x) \in R^{7\times 1}$, $g(x) \in R^{7\times 4}$ and $u \in R^{4\times 1}$. The associated matrix equations are given next

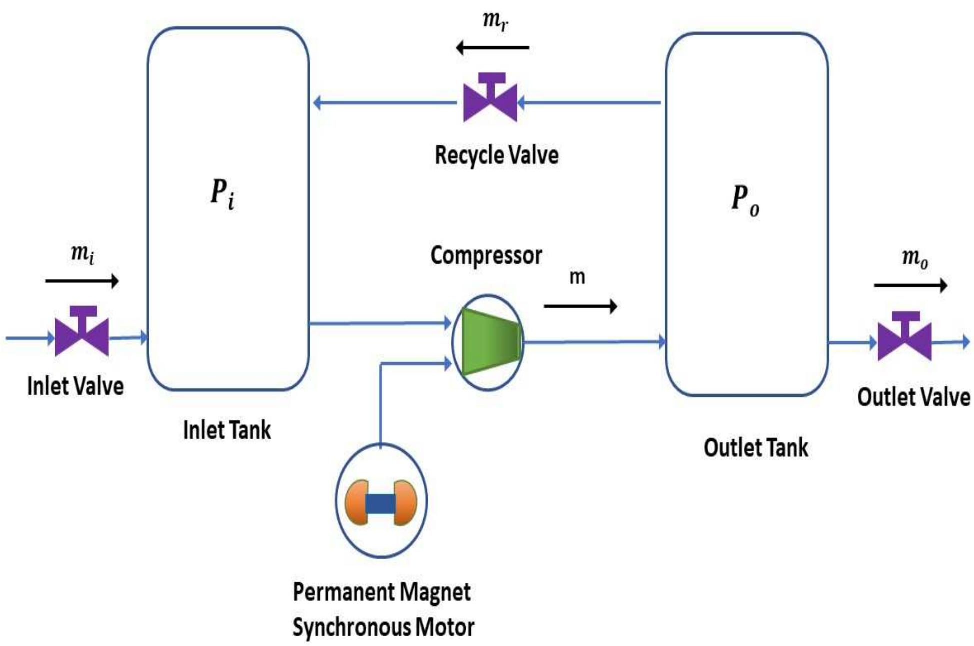

Figure 2: Diagram of the PMSM electrically-driven gas compressor

$$f(x) = \begin{pmatrix} \frac{a_i^2}{V_i}[-x_3 + x_5] \\ \frac{a_o^2}{V_o}[-K_o\sqrt{x_2 - p_{atm}} + x_3 - x_5] \\ \frac{1}{L}[\pi(x_3, x_4)x_1 - x_2] \\ \frac{1}{J}\{[px_7(\Psi_m) - (L_d - L_q)x_6] - \tau_c(x_3, x_4) - vx_4\} \\ 0 \\ \frac{1}{L_d}(-Rx_6 - px_4 L_q x_7) \\ \frac{1}{L_q}(-Rx_7 - px_4 L_d x_6 - x_4\Psi_m) \end{pmatrix} \tag{79}$$

$$g(x) = \begin{pmatrix} \frac{a_i^2}{V_i}\sqrt{p_{atm} - x_1} & 0 & 0 & 0 \\ 0 & 0 & 0 & 0 \\ 0 & 0 & 0 & 0 \\ 0 & 0 & 0 & 0 \\ -\frac{1}{T_r}\sqrt{p_{atm} - x_1} & \frac{1}{T_r}\sqrt{x_2 - x_1} & 0 & 0 \\ 0 & 0 & \frac{1}{L_d} & 0 \\ 0 & 0 & 0 & \frac{1}{L_q} \end{pmatrix} \tag{80}$$

4.2 State-space model of the PMSM-driven gas-compressor

The state vector of the PMSM-driven gas-compressor is given by:

$$x = [x_1, x_2, x_3, x_4, x_5, x_6, x_7]^T = [P_1, P_2, m, \omega, m_r, i_d, i_q]^T \tag{81}$$

and the control inputs vector is given by

$$u = [u_1, u_2, u_3, u_4]^T = [K_i, K_r, v_d, v_q]^T \tag{82}$$

The dynamic model of the PMSM-driven gas compressor is given by

$$\begin{pmatrix} \dot{x}_1 \\ \dot{x}_2 \\ \dot{x}_3 \\ \dot{x}_4 \\ \dot{x}_5 \\ \dot{x}_6 \\ \dot{x}_7 \end{pmatrix} = \begin{pmatrix} \frac{a_i^2}{V_i}(-x_3 + x_5) \\ \frac{a_o^2}{V_o}(-K_o\sqrt{x_2 - p_{atm}} + x_3 - x_5) \\ \frac{1}{L}[\pi(x_3, x_4)x_1 - x_2] \\ \frac{1}{J}\{[px_7\Psi_m - (L_d - L_q)x_6] - \tau_c(x_3, x_4) - vx_4\} \\ 0 \\ \frac{1}{L_d}(-Rx_6 - px_4L_qx_7) \\ \frac{1}{L_q}(-Rx_7 - px_4L_dx_6 - x_4\Psi_m) \end{pmatrix} + \begin{pmatrix} \frac{a_i^2}{V_i}\sqrt{p_{atm - x_1}} & 0 & 0 & 0 \\ 0 & 0 & 0 & 0 \\ 0 & 0 & 0 & 0 \\ 0 & 0 & 0 & 0 \\ -\frac{1}{T_r}\sqrt{p_{atm} - x_1} & \frac{1}{T_r}\sqrt{x_2 - x_1} & 0 & 0 \\ 0 & 0 & \frac{1}{L_d} & 0 \\ 0 & 0 & 0 & \frac{1}{L_q} \end{pmatrix} \begin{pmatrix} u_1 \\ u_2 \\ u_3 \\ u_4 \end{pmatrix} \tag{83}$$

Next, the system's state-space model is reorganized as follows:

$$\dot{x}_2 = \frac{a_o^2}{V_o}(-K_o\sqrt{x_2 - p_{atm}} + x_3 - x_5) \tag{84}$$

$$\dot{x}_3 = \frac{1}{L}[\pi(x_3, x_4)z_1 - x_2] \tag{85}$$

$$\dot{x}_1 = \frac{a_i^2}{V_i}(-x_3 + x_5) + \frac{a_i^2}{V_i}\sqrt{p_{atm - x_1}}u_1 \tag{86}$$

$$\dot{x}_5 = -\frac{1}{T_r}\sqrt{p_{atm} - x_1}u_1 + \frac{1}{T_r}\sqrt{x_2 - x_1}u_2 \tag{87}$$

$$\dot{x}_4 = \frac{1}{J}\{[px_7\Psi_m - (L_d - L_q)x_6] - \tau_c(x_3, x_4) - vx_4\} \tag{88}$$

$$\dot{x}_6 = \frac{1}{L_d}(-Rx_6 - px_4L_qx_7) + \frac{1}{L_d}u_3 \tag{89}$$

$$\dot{x}_7 = \frac{1}{L_q}(-Rx_7 - px_4L_dx_6 - x_4\Psi_m) + \frac{1}{L_q}u_4 \tag{90}$$

Next, the state variables of the system are re-defined as: $z_1 = x_2$, $z_2 = x_3$, $z_3 = x_1$, $z_4 = x_5$, $z_5 = x_4$, $z_6 = x_6$ and $z_7 = x_7$. Using this state variables notation the system's state-space model is rewritten as::

$$\dot{z}_1 = \frac{a_o^2}{V_o}(-K_o\sqrt{z_3 - p_{atm}} + z_2 - z_4) \tag{91}$$

$$\dot{z}_2 = \frac{1}{L}[\pi(z_2, z_5)z_3 - z_1] \tag{92}$$

$$\dot{z}_3 = \frac{a_i^2}{V_i}(-z_2 + z_4) + \frac{a_i^2}{V_i}\sqrt{p_{atm - z_3}}u_1 \tag{93}$$

$$\dot{z}_4 = -\frac{1}{T_r}\sqrt{p_{atm} - z_3}u_1 + \frac{1}{T_r}\sqrt{z_1 - z_3}u_2 \tag{94}$$

$$\dot{z}_5 = \frac{1}{J}\{[pz_7\Psi_m - (L_d - L_q)z_6] - \tau_c(z_2, z_5) - vz_5\} \tag{95}$$

$$\dot{z}_6 = \frac{1}{L_d}(-Rz_6 - pz_5L_qz_7) + \frac{1}{L_d}u_3 \tag{96}$$

$$\dot{z}_7 = \frac{1}{L_q}(-Rz_7 - pz_5 L_d z_6 - z_5 \Psi_m) + \frac{1}{L_q}u_4 \tag{97}$$

Next, the dynamics of the PMSM-driven gas-compressor is written in the form of the following chained subsystems:

$$\begin{pmatrix} \dot{z}_1 \\ \dot{z}_2 \end{pmatrix} = \begin{pmatrix} \frac{a_o^2}{V_o}(-K_o\sqrt{z_3 - p_{atm}} + z_2) \\ -\frac{1}{L}z_1 \end{pmatrix} + \begin{pmatrix} 0 & -\frac{a_o^2}{V_o} \\ -\frac{1}{L}\pi(z_2, z_5) & 0 \end{pmatrix} \begin{pmatrix} z_3 \\ z_4 \end{pmatrix} \tag{98}$$

$$\begin{pmatrix} \dot{z}_3 \\ \dot{z}_4 \end{pmatrix} = \begin{pmatrix} \frac{a_i^2}{V_i}(-z_2 + z_4) \\ 0 \end{pmatrix} + \begin{pmatrix} -\frac{a_i^2}{V_i}\sqrt{p_{atm} - z_1} & 0 \\ -\frac{1}{T_r}\sqrt{p_{atm} - z_3} & \frac{1}{T_r}\sqrt{z_1 - z_3} \end{pmatrix} \begin{pmatrix} u_1 \\ u_2 \end{pmatrix} \tag{99}$$

$$\dot{z}_5 = [-\tfrac{1}{J}\tau_c(z_2, z_5) - \tfrac{v}{J}z_5] + [\tfrac{L_d - L_q}{J}z_6 + \tfrac{p\Psi_m}{J}z_7] \tag{100}$$

$$\begin{pmatrix} z_6 \\ z_7 \end{pmatrix} = \begin{pmatrix} \frac{1}{L_d}(-Rz_6 - pz_5 L_q z_7) \\ \frac{1}{L_q}(-Rz_7 - pz_5 L_d z_6 - z_5\Psi_m) \end{pmatrix} + \begin{pmatrix} \frac{1}{L_d} & 0 \\ 0 & \frac{1}{L_q} \end{pmatrix} \begin{pmatrix} u_3 \\ u_4 \end{pmatrix} \tag{101}$$

4.3 Differential flatness-properties of the PMSM-driven gas-compressor

The dynamic system of the PMSM-driven gas-compressors is differentially flat with flat outputs vector

$$Y = [y_1, y_2, y_3, y_4]^T = [x_1, x_2, x_4, x_6]^T = [z_3, z_1, z_2, z_6]^T \tag{102}$$

From the first row of the re-arranged state-space model one has:

$$\dot{z}_1 = \frac{a_0^2}{V_o}(-K_o\sqrt{z_1 - p_{atm}} + z_2 - z_4) \tag{103}$$

and by solving for z_4 it holds that

$$z_4 = \frac{1}{a_o^2}[-V_o\dot{z}_1 - a_o^2 K_o\sqrt{z_1 - p_{atm}} + a_o^2 z_2] \tag{104}$$

which signifies that z_4 is a differential function of the flat output of the system or $z_4 = h_4(Y, \dot{Y})$. From the second row of the re-arranged state-space model one has

$$\dot{z}_2 = \frac{1}{L}[\pi(z_2, z_5)z_3 - z_1] \tag{105}$$

thus, by solving for z_5 it holds that

$$\pi(z_2, z_5) = \frac{1}{z_3}[L\dot{z}_2 + z_1] \tag{106}$$

which allows for expressing z_5 in the form of a differential function of the flat output vector, or $z_5 = h_5(Y, \dot{Y})$. From the fifth row of the state-space model one has

$$\dot{z}_5 = \frac{1}{J}[pz_7\Psi_m - (L_d - L_q)z_6] - \tau_c(z_2, z_5) - vz_6 \tag{107}$$

thus by solving for z_7 one has

$$z_7 = \frac{1}{p\Psi_m}[J\dot{z}_5 + (L_d - L_q)z_6 + \tau_c(z_3, z_4) + vz_5] \tag{108}$$

which signifies that z_7 is a differential function of the flat outputs vector Y or $z_7 = h_7(Y, \dot{Y})$. Next, from the 3rd, 4th, 6th and 7th rows of the state-space model one has the following system of equations

$$\begin{pmatrix} \dot{z}_3 \\ \dot{z}_4 \\ \dot{z}_6 \\ \dot{z}_7 \end{pmatrix} = \begin{pmatrix} \frac{a_i^2}{V_i}(-z_2+z_4) \\ 0 \\ \frac{1}{L_d}(-Rz_6 - pz_5L_qz_7) \\ \frac{1}{L_q}(-Rz_7 - pz_5L_dz_6 - z_5\Psi_m) \end{pmatrix} + \begin{pmatrix} \frac{a_i^2}{V_i} & 0 & 0 & 0 \\ -\frac{1}{T_r}\sqrt{p_{atm}-z_3} & \frac{1}{T_r}\sqrt{z_1-z_3} & 0 & 0 \\ 0 & 0 & \frac{1}{L_d} & 0 \\ 0 & 0 & 0 & \frac{1}{L_q} \end{pmatrix} \begin{pmatrix} u_1 \\ u_2 \\ u_3 \\ u_4 \end{pmatrix} \tag{109}$$

or, in concise form the previous matrix equation is written as

$$\dot{\tilde{z}} = \tilde{f} + \tilde{g}u \Rightarrow u = \tilde{g}^1[\dot{\tilde{z}} - \tilde{F}] \tag{110}$$

where $\tilde{z}$, $\tilde{f}$, $\tilde{g}$, are differential functions of the flat outputs vector. Thus it is also inferred that u is also a differential function of the flat outputs vector Y, or equivalently $u = h_u(Y, \dot{Y})$. Consequently, the dynamic model of the PMSM-driven gas compressor is differentially flat. The differential flatness properties of this system confirm its linearizability and implicitly also its controllability.

5 Flatness-based control in successive loops for the PMSM-driven gas-compressor

It will be proven that each one of the subsystems of Eq. (98) to Eq. (101) is differentially flat and a flatness-based controller can be designed about it. The following sub-vectors and sub-matrices are defined: For subsystem Σ_1 one has subvector $z_{1,2}$ and submatrices $f_{1,2}(z_{1,2})$, $g_{1,2}(z_{1,2})$ and virtual control input $v_1 = [v_3, v_4]^T$:

$$\dot{z}_{1,2} = \begin{pmatrix} z_1 \\ z_2 \end{pmatrix} \quad f_{1,2} = \begin{pmatrix} \frac{a_o^2}{V_o}(-K_o\sqrt{z_1 - p_{atm}} + z_2) \\ -\frac{1}{L}z_1 \end{pmatrix} \quad g_{1,2} = \begin{pmatrix} 0 & -\frac{a_o^2}{V_o} \\ -\frac{1}{L}\pi(z_2, z_5) & 0 \end{pmatrix} \tag{111}$$

For subsystem Σ_2 one has subvector $z_{3,4}$ and submatrices $f_{3,4}(z_{1,2}, z_{3,4})$, $g_{3,4}(z_{1,2}, z_{3,4})$ and real control input $u_a = [u_1, u_2]^T$:

$$z_{3,4} = \begin{pmatrix} z_3 \\ z_4 \end{pmatrix} \quad f_{3,4} = \begin{pmatrix} \frac{a_i^2}{V_i}(-z_2 + z_4) \\ 0 \end{pmatrix} \quad g_{3,4} = \begin{pmatrix} -\frac{a_i^2}{V_i}\sqrt{p_{atm} - z_1} & 0 \\ -\frac{1}{T_r}\sqrt{p_{atm} - z_3} & \frac{1}{T_r}\sqrt{z_1 - z_3} \end{pmatrix} \tag{112}$$

For subsystem Σ_3 one has subvector z_5 and submatrices $f_5(z_{1,2}, z_{3,4}, z_5)$, $g_5(z_{1,2}, z_{3,4}, z_5)$ and virtual control input $v_2 = -\frac{(L_d - L_q)}{J}z_6 + \frac{\mu\Psi_m}{J}z_7$:

$$z_5 \quad f_5 = -\frac{1}{J}\tau_c(z_2, z_5) - \frac{v}{J}z_5 \quad g_5 = 1 \tag{113}$$

For subsystem Σ_4 one has subvector $z_{6,7}$ and submatrices $f_{6,7}(z_{1,2}, z_{3,4}, z_5, z_{6,7})$, $g_{6,7}(z_{1,2}, z_{3,4}, z_5, z_{6,7})$ and real control input $u_b = [u_3, u_4]^T$:

$$z_{6,7} = \begin{pmatrix} z_6 \\ z_7 \end{pmatrix} \quad f_{6,7} = \begin{pmatrix} \frac{1}{L_d}(-Rz_6 - pz_5L_qz_7) \\ \frac{1}{L_q}(-Rz_7 - pz_5L_dz_6 - z_5\Psi_m) \end{pmatrix} \quad g_{6,7} = \begin{pmatrix} \frac{1}{L_d} & 0 \\ 0 & \frac{1}{L_q} \end{pmatrix} \tag{114}$$

Thus, the dynamics of the PMSM-driven gas-compressor can be written in the form of the following subsystems Σ_1 to Σ_4:

$$\dot{z}_{1,2} = f_{1,2}(z_{1,2}) + g_{1,2}(z_{1,2})v_1 \tag{115}$$

$$\dot{z}_{3,4} = f_{3,4}(z_{1,2}, z_{3,4}) + g_{3,4}(z_{1,2}, z_{3,4})u_a \tag{116}$$

$$\dot{z}_5 = f_5(z_{1,2}, z_{3,4}, z_5) + g_5(z_{1,2}, z_{3,4}, z_5)v_2 \tag{117}$$

$$\dot{z}_{6.7} = f_{6,7}(z_{1,2}, z_{3,4}, z_5, z_{6,7}) + g_{6,7}(z_{1,2}, z_{3,4}, z_5, z_{6,7})u_b \tag{118}$$

For the subsystem Σ_1 of Eq. (115) the flat output is defined as $y_1 = z_{1,2}$ and the virtual control input is $v_1 = z_{3,4}$. By solving Eq. (115) for v_1 one has

$$v_1 = g_{1,2}(z_{1,2})^{-1}[\dot{z}_{1,2} - f_{1,2}(z_{1,2})] \tag{119}$$

which signifies that v_1 is a differential function of the flat output y_1 and that the subsystem of Eq. (115) is differentially flat.

For the subsystem Σ_2 of Eq. (115) the flat output is defined as $y_2 = z_{3,4}$, the real control input is u_a, while $z_{1,2}$ is viewed as a coefficients vector. By solving for u_a one has

$$u_a = g_{3,4}(z_{1,2}, z_{3,4})^{-1}[\dot{z}_{3,4} - f_{3,4}(z_{1,2}, z_{3,4})] \tag{120}$$

which signifies that u_a is a differential function of the flat output y_2, and thus the subsystem of Eq. (116) is differentially flat.

For the subsystem Σ_3 of Eq. (117) the flat outputs vector is $y_3 = z_5$, the virtual control input is v_2 while $z_{1,2}$ and $z_{3,4}$ are viewed as coefficients. Solving Eq. (117) for v_2 gives

$$v_2 = g_5(z_{1,2}, z_{3,4}, z_5)^{-1}[\dot{z}_5 - f_5(z_{1,2}, z_{3,4}, z_5)] \tag{121}$$

which signifies that v_2 is a differential function of the flat output y_3 and that the subsystem of Eq. (117) is differentially flat.

For the subsystem Σ_4 of Eq. (118) the flat output vector is $y_4 = z_{6,7}$, the real control input is u_b, while $z_{1,2}$, $z_{3,4}$, z_5 are viewed as coefficients. By solving Eq. (118) for v_b one obtains

$$u_b = g_{6,7}(z_{1,2}, z_{3,4}, z_5, z_{6,7})^{-1}[\dot{z}_{6,7} - f_{6,7}(z_{1,2}, z_{3,4}, z_5, z_{6,7})] \tag{122}$$

which signifies that u_b is a differential function of the flat output y_4 and that the subsystem of Eq. (118) is differentially flat.

Knowing that each one of the subsystems Σ_1 to Σ_4 of Eq. (115) to Eq. (118) is differentially flat means also that each one of them can be written in the input-output linearized form. Besides, it means that a stabilizing feedback controller can be designed for each one of these subsystems by applying inversion of its dynamics, as it is usually done for input-output linearized systems.

For the subsystem Σ_1 of Eq. (115) the stabilizing feedback control is taken to be $v_1 = z_{1.2}^d$

$$v_1 = g_{1,2}(z_{1,2})[\dot{z}_{1,2}^d - f_{1,2}(z_{1,2}) - K_1(z_{1,2} - z_{1,2}^d)] \tag{123}$$

where $K_1 > 0$ is a diagonal matrix with diagonal elements $k_{1,ii} > 0$ for $i = 1, 2$. The virtual control input $v_1 = z_{1,2}^d$ becomes setpoint to the subsystem of Eq. (116). For the subsystem Σ_2 of Eq. (116) the stabilizing feedback control is taken to be

$$u_a = g_{3,4}(z_{1,2}, z_{3,4})[\dot{z}_{3,4}^d - f_{3,4}(z_{1,2}, z_{3,4}) - K_2(z_{3,4} - z_{3,4}^d)] \tag{124}$$

where $K_2 > 0$ is a diagonal matrix with diagonal elements $k_{2,ii} > 0$ for $i = 1, 2$. For the subsystem Σ_3 of Eq. (117) the stabilizing feedback control is taken to be

$$v_2 = g_5(z_{1,2}, z_{3,4}, z_5)[\dot{z}_5^d - f_5(z_{1,2}, z_{3,4}, z_5) - K_3(z_5 - z_5^d)] \tag{125}$$

where $K_3 > 0$ is a positive scalar feedback gain. Knowing that the desirable value for control input v_2 is $v_2^* = -\frac{(L_d - L_q)}{J} z_6 + \frac{\mu \Psi_m}{J} z_7$ and by assigning a desirable setpoint value to z_6 which is denoted as z_6^d one can also find the desirable (setpoint) value for z_7 which is denoted as z_7^d. Actually it holds that

$$z_7^d = \frac{1}{p\Psi_m}[Jv_2^* + (L_d - L_q)z_6^d] \tag{126}$$

For the subsystem Σ_4 of Eq. (118) the stabilizing feedback control is taken to be

$$u_b = g_{6,7}(z_{1,2}, z_{3,4}, z_{5,6}, z_7)[\dot{z}_{6,7}^d - f_{6,7}(z_{1,2}, z_{3,4}, z_{5,6}, z_7) - K_4(z_{6,7} - z_{6,7}^d)] \tag{127}$$

where $K_4 > 0$ is a diagonal matrix with diagonal elements $k_{4,ii} > 0$ for $i = 1, 2$. The setpoints vector $z_{6,7}^d = [z_6^d, z_7^d]$ has been defined before using the value of z_6^d and the value of z_7^d that was computed from Eq. (126).

Next, the following tracking error variables are defined: $e_{1,2} = z_{1,2} - z_{1,2}^d$, $e_{3,4} = z_{3,4} - z_{3,4}^d$, $e_5 = z_5 - z_5^d$, $e_{6,7} = z_{6,7} - z_{6,7}^d$.. By substituting Eq. (123) into Eq. (115) the following tracking error dynamics is obtained

$$\begin{array}{c} \dot{z}_{1,2} = f_{1,2}(z_{1,2}) + g_{1,2}(z_{1,2})g_{1,2}(z_{1,2})^{-1}[\dot{z}_{1,2}^d - f_{1,2}(z_{1,2}) - K_1(z_{1,2} - z_{1,2}^d)] \Rightarrow \\ (\dot{z}_{1,2} - \dot{z}_{1,2}^d) + K_1(z_{1,2} - z_{1,2}^d) = 0 \Rightarrow \dot{e}_{1,2} + K_1 e_{1,2} = 0 \Rightarrow \\ lim_{t\to\infty} e_{1,2}(t) = 0 \Rightarrow lim_{t\to\infty} z_{1,2}(t) = z_{1,2}^d(t) \end{array} \tag{128}$$

By substituting Eq. (124) into Eq. (116) the following tracking error dynamics is obtained

$$\begin{array}{c} \dot{z}_{3,4} = f_{3,4}(z_{1,2}, z_{3,4}) + g_{3,4}(z_{1,2}, z_{3,4})g_{1,2}(z_{1,2}, z_{3,4})^{-1}[\dot{z}_{3,4}^d - f_{3,4}(z_{1,2}, z_{3,4}) - K_2(z_{3,4} - z_{3,4}^d)] \Rightarrow \\ (\dot{z}_{3,4} - \dot{z}_{3,4}^d) + K_2(z_{3,4} - z_{3,4}^d) = 0 \Rightarrow \dot{e}_{3,4} + K_2 e_{3,4} = 0 \Rightarrow \\ lim_{t\to\infty} e_{3,4}(t) = 0 \Rightarrow lim_{t\to\infty} z_{3,4}(t) = z_{3,4}^d(t) \end{array} \tag{129}$$

By substituting Eq. (125) into Eq. (117) the following tracking error dynamics is obtained

$$\begin{array}{c} \dot{z}_5 = f_5(z_{1,2}, z_{3,4}, z_5) + g_5(z_{1,2}, z_{3,4}, z_5)g_5(z_{1,2}, z_{3,4}, z_5)^{-1}[\dot{z}_5^d - f_5(z_{1,2}, z_{3,4}, z_5) - K_3(z_5 - z_5^d)] \Rightarrow \\ (\dot{z}_5 - \dot{z}_5^d) + K_3(z_5 - z_5^d) = 0 \Rightarrow \dot{e}_5 + K_3 e_5 = 0 \Rightarrow \\ lim_{t\to\infty} e_5(t) = 0 \Rightarrow lim_{t\to\infty} z_5(t) = z_5^d(t) \end{array} \tag{130}$$

Finally, by substituting Eq. (127) into Eq. (118) the following tracking error dynamics is obtained

$$\begin{array}{c} \dot{z}_{6,7} = f_{6,7}(z_{1,2}, z_{3,4}, z_5, z_{6,7}) + g_{6,7}(z_{1,2}, z_{3,4}, z_5, z_{6,7})g_{6,7}(z_{1,2}, z_{3,4}, z_5, z_{6,7})^{-1} \\ \cdot[\dot{z}_{6,7}^d - f_{6,7}(z_{1,2}, z_{3,4}, z_5, z_{6,7}) - K_4(z_{6,7} - z_{6,7}^d)] \Rightarrow \\ (\dot{z}_{6,7} - \dot{z}_{6,7}^d) + K_4(z_{6,7} - z_{6,7}^d) = 0 \Rightarrow \dot{e}_{6,7} + K_4 e_{6,7} = 0 \Rightarrow \\ lim_{t\to\infty} e_{6,7}(t) = 0 \Rightarrow lim_{t\to\infty} z_{6,7}(t) = z_{6,7}^d(t) \end{array} \tag{131}$$

By proving that state vector elements z_i converge to the associated setpoints z_i^d it is also proven that the state variables of the initial nonlinear system x_i converge to their setpoints x_i^d. Thus, the control loop of the PMSM-driven gas compressor is globally asymptotically stable.

Global stability can be also proven through Lyapunov analysis. To this end, the following Lyapunov function is defined:

$$V = \frac{1}{2}[e_{1,2}^T e_{1,2} + e_{3,4}^T e_{3,4} + e_5^2 + e_{6,7}^T e_{6,7}] \tag{132}$$

By differentiating the above equation in time one obtains:

$$\dot{V} = \frac{1}{2}2[e_{1,2}^T \dot{e}_{1,2} + e_{3,4}^T \dot{e}_{3,4} + e_5 \dot{e}_5 + e_{6,7}^T \dot{e}_{6,7}] \tag{133}$$

Next, by substituting in Eq. (133) the relations about the tracking error dynamics which are provided by Eq. (128) to Eq. (131) one gets

$$\begin{array}{c}\dot{V}=[e_{1,2}^T(-K_1e_{1,2})+e_{3,4}^T(-K_2e_{3,4})+e_5(-K_3e_5)+e_{6,7}^T(-K_4e_{6,7})]\Rightarrow\\ \dot{V}=-[e_{1,2}^T(K_1e_{1,2})+e_{3,4}^T(K_2e_{3,4})+(K_3e_5^2)+e_{6,7}^T(K_4e_{6,7})]\Rightarrow\\ \dot{V}<0\ \forall\ e_{1,2}\neq 0,\ e_{3,4}\neq 0,\ e_5\neq 0,\ e_{6,7}\neq 0,\end{array} \tag{134}$$

and $\dot{V}=0$ if and only if $e_{1,2}=0$, $e_{3,4}=0$, $e_5=0$ and $e_{6,7}=0$. Consequently, Lyapunov function V is a strictly diminishing function which converges asymptotically to the fixed point $[e_{1,2}^T=0_{1\times 2}, e_{3,4}^T=0_{1\times 2}, e_5=0, e_{6,7}^T=0_{1\times 2}]$. In this manner, it is proven once again that the dynamic model of the PMSM-driven gas compressor is globally asymptotically stable.

6 Simulation tests

6.1 Results on control of IM-driven gas compressors

Results about the tracking accuracy and the speed of convergence to setpoints of the successive-loops flatness-based control method, in the case of the induction motor-driven gas compressor, are shown in Fig. 3 to Fig. 18. A per-unit (p.u.) state variables notation has been used. It can be noticed, that under this control scheme one achieves fast and precise tracking of reference setpoints for all state variables of the induction motor-driven gas compressor. It is noteworthy, that through the stages of this method one solves also the setpoints definition problem for all state variables of the induction motor-driven gas compressor. Actually, the selection of setpoints for state variables x_2, x_3, x_4 and x_6 is unconstrained. On the other side by defining state variables x_1, x_5, x_6, x_7 as virtual control inputs to the subsystem of x_2, x_3, x_4, x_6 one can find the setpoints for x_1, x_5, x_6, x_7 as functions of the setpoints for x_2, x_3, x_4, x_6. The speed of convergence of the state variables of the induction motor-driven gas compressor under flatness-based control implemented in successive loops is dependent on the selection of values for the diagonal gain matrices K_i, $i=1,2$ of Eq. (59) to Eq. (60).

6.2 Results on control of PMSM-driven gas compressor

Results about the tracking accuracy and the speed of convergence to setpoints of the successive-loops flatness-based control method, in the case of the PMSM-driven gas compressor, are shown in Fig. 19 to Fig. 34. A per-unit (p.u.) state variables notation has been used. It can be noticed, that under this control scheme one achieves fast and precise tracking of reference setpoints for all state variables of the PMSM-driven gas compressor. It is noteworthy, that through the stages of this method one solves also the setpoints definition problem for all state variables of the PMSM-driven gas compressor. Actually, the selection of setpoints for state variables x_2 and x_3 is unconstrained. On the other side by defining state variables x_1 and x_5 as virtual control inputs for the subsystem of x_2, x_3 one can find the setpoints for x_1, x_5 as functions of the setpoints for x_2, x_3. In a similar manner the selection of setpoints for the turn speed x_4 of the compressor is unconstrained. On the other side by defining state variables x_6 and x_7 as parts of the virtual control input for the subsystem of x_2, and by assigning without constraints a value to the setpoint of x_6 one can also find the setpoinf for x_7 as a function of the setpoints of x_4, x_6. The speed of convergence of the state variables of the PMSM-driven gas compressor under flatness-based control implemented in successive loops is dependent on the selection of values for the diagonal gain matrices K_i, $i=1,\cdots,4$ of Eq. (123) to Eq. (123) .

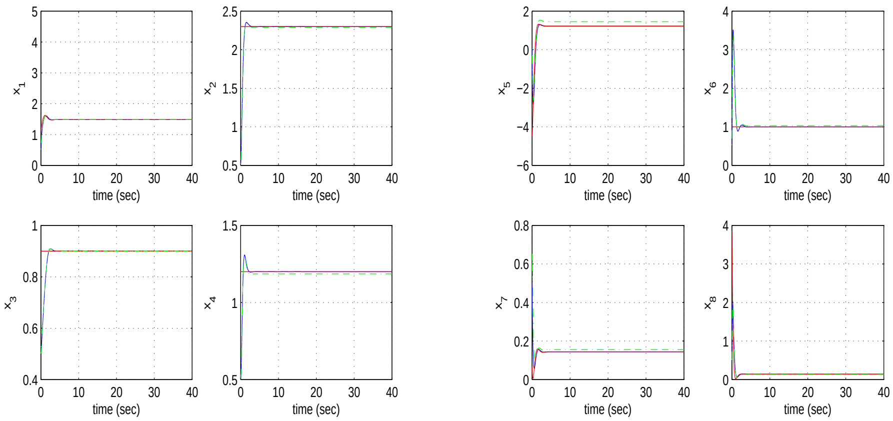

(a) **(b)**

Figure 3: Tracking of setpoint 1 by the induction motor-driven gas compressor (a) Convergence of state variables x_1 to x_4 (blue lines) to the reference setpoints (red lines) and their KF-based estimation (green line), (b) Convergence of state variables x_5 to x_8 (blue lines) to the reference setpoints (red lines) and their KF-based estimation (green line)

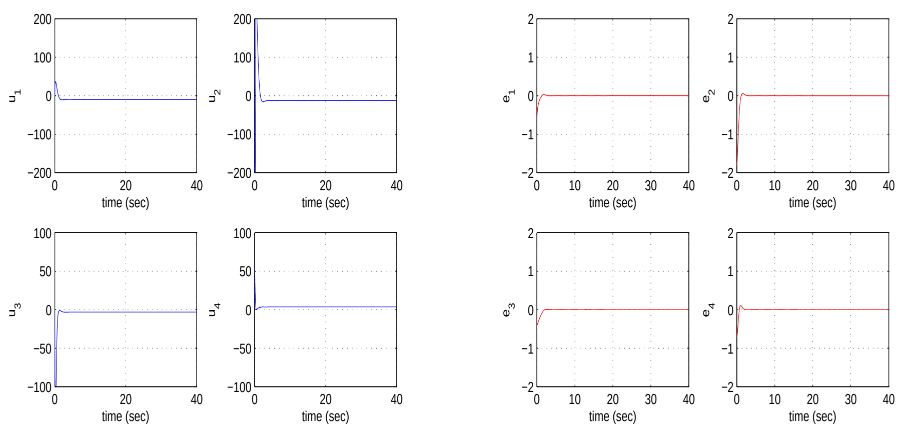

(a) **(b)**

Figure 4: Tracking of setpoint 1 by the induction motor-drive gas compressor (a) Variations of the control inputs u_1 to u_4, (b) Tracking error of state variables x_1 to x_4

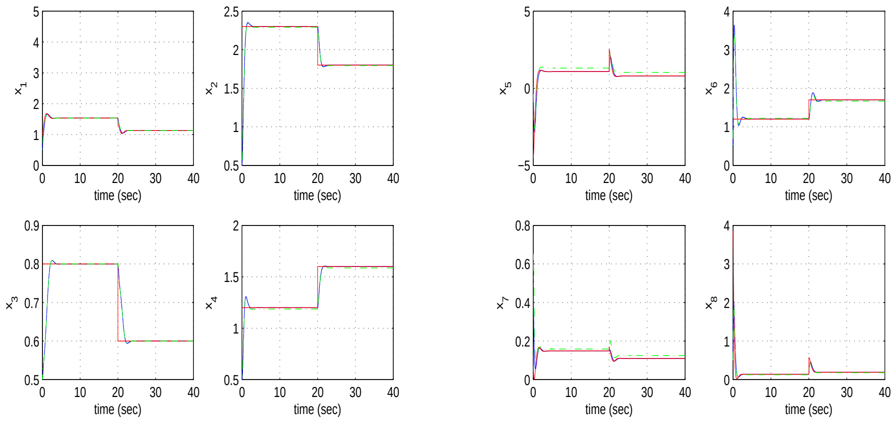

(a) **(b)**

Figure 5: Tracking of setpoint 2 by the induction motor-driven gas compressor (a) Convergence of state variables x_1 to x_4 (blue lines) to the reference setpoints (red lines) and their KF-based estimation (green line), (b) Convergence of state variables x_5 to x_8 (blue lines) to the reference setpoints (red lines) and their KF-based estimation (green line)

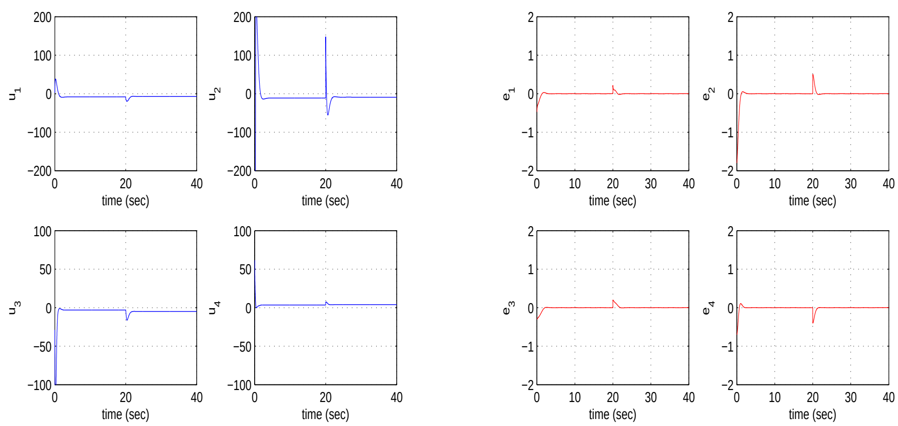

(a) **(b)**

Figure 6: Tracking of setpoint 2 by the induction motor-drive gas compressor (a) Variations of the control inputs u_1 to u_4, (b) Tracking error of state variables x_1 to x_4

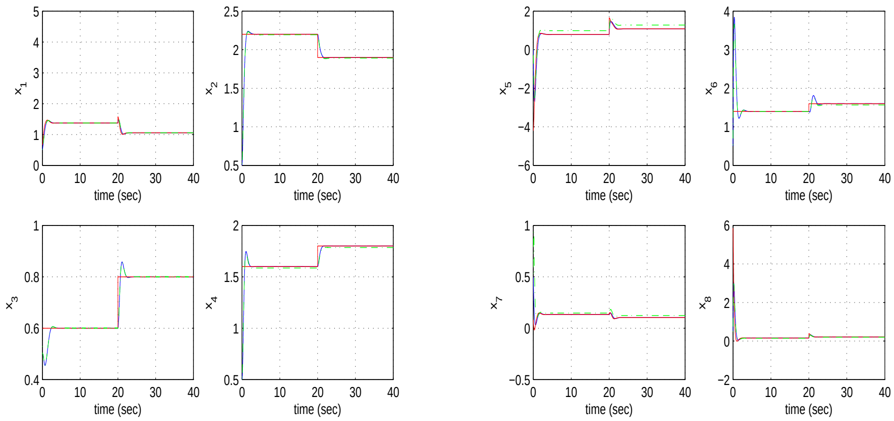

(a) **(b)**

Figure 7: Tracking of setpoint 3 by the induction motor-driven gas compressor (a) Convergence of state variables x_1 to x_4 (blue lines) to the reference setpoints (red lines) and their KF-based estimation (green line), (b) Convergence of state variables x_5 to x_8 (blue lines) to the reference setpoints (red lines) and their KF-based estimation (green line)

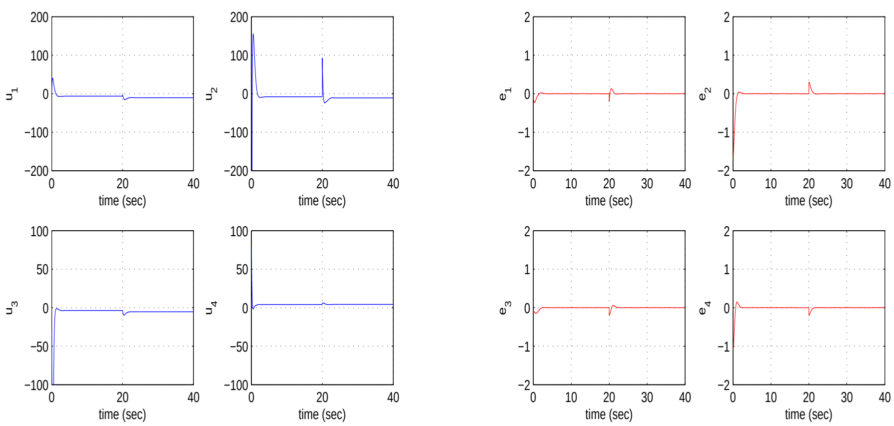

(a) **(b)**

Figure 8: Tracking of setpoint 3 by the induction motor-drive gas compressor (a) Variations of the control inputs u_1 to u_4, (b) Tracking error of state variables x_1 to x_4

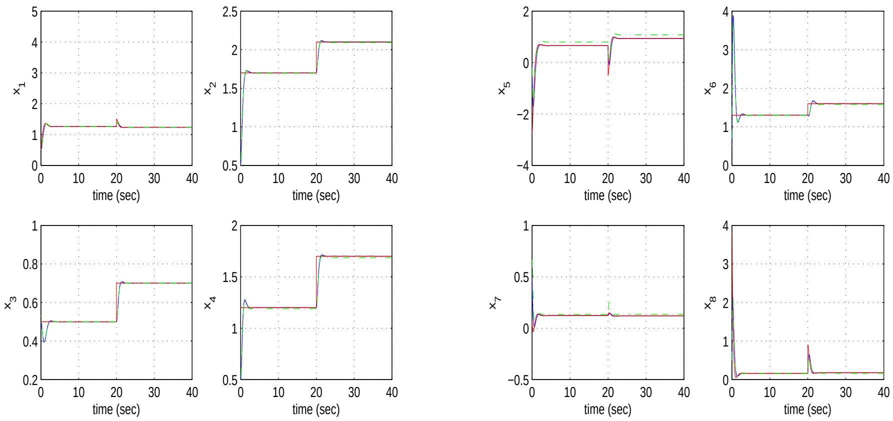

(a) **(b)**

Figure 9: Tracking of setpoint 4 by the induction motor-driven gas compressor (a) Convergence of state variables x_1 to x_4 (blue lines) to the reference setpoints (red lines) and their KF-based estimation (green line), (b) Convergence of state variables x_5 to x_8 (blue lines) to the reference setpoints (red lines) and their KF-based estimation (green line)

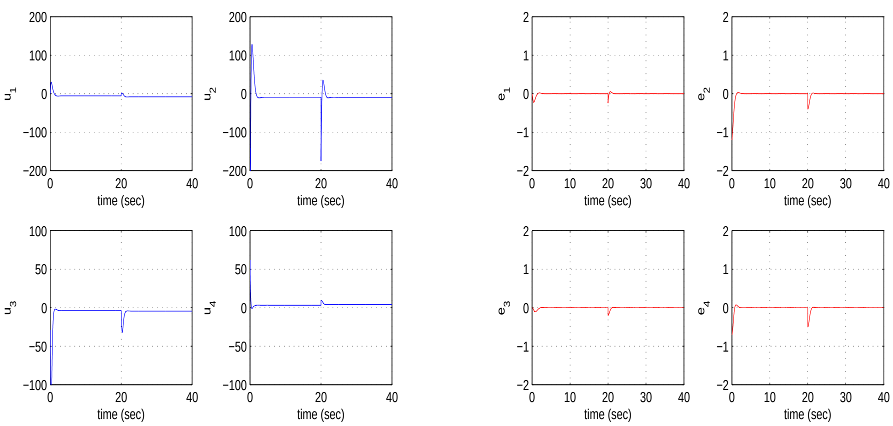

(a) **(b)**

Figure 10: Tracking of setpoint 4 by the induction motor-drive gas compressor (a) Variations of the control inputs u_1 to u_4, (b) Tracking error of state variables x_1 to x_4

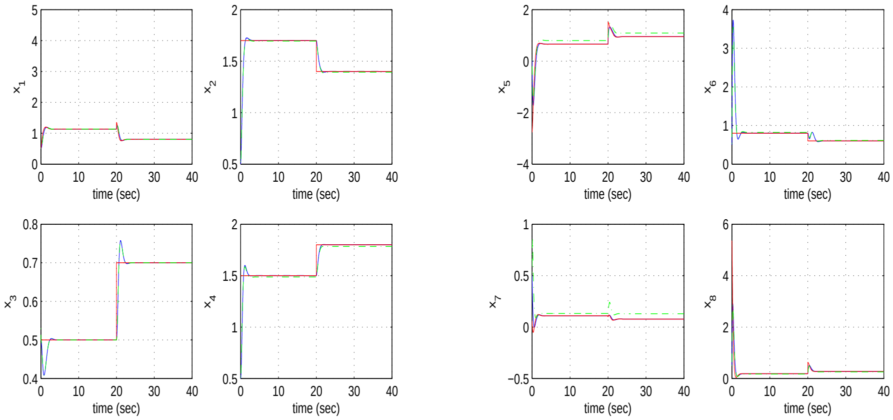

(a) **(b)**

Figure 11: Tracking of setpoint 5 by the induction motor-driven gas compressor (a) Convergence of state variables x_1 to x_4 (blue lines) to the reference setpoints (red lines) and their KF-based estimation (green line), (b) Convergence of state variables x_5 to x_8 (blue lines) to the reference setpoints (red lines) and their KF-based estimation (green line)

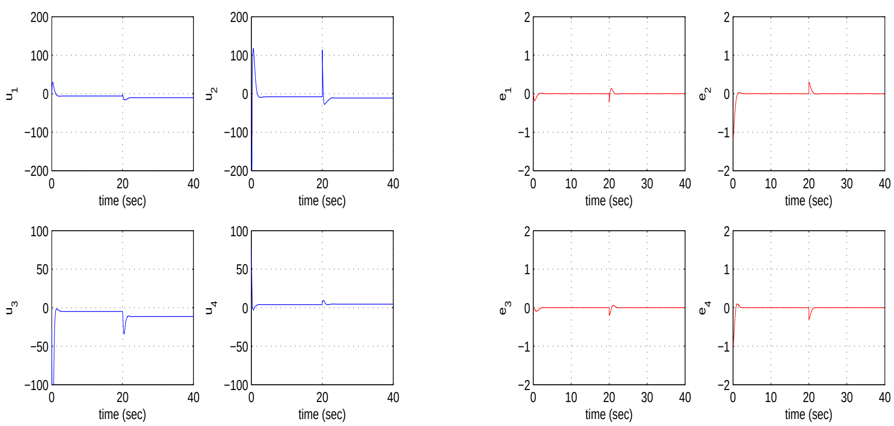

(a) **(b)**

Figure 12: Tracking of setpoint 5 by the induction motor-drive gas compressor (a) Variations of the control inputs u_1 to u_4, (b) Tracking error of state variables x_1 to x_4

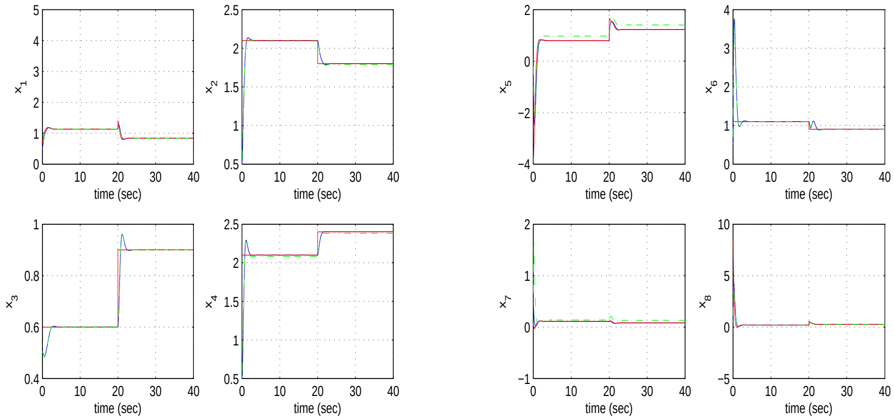

(a) **(b)**

Figure 13: Tracking of setpoint 6 by the induction motor-driven gas compressor (a) Convergence of state variables x_1 to x_4 (blue lines) to the reference setpoints (red lines) and their KF-based estimation (green line), (b) Convergence of state variables x_5 to x_8 (blue lines) to the reference setpoints (red lines) and their KF-based estimation (green line)

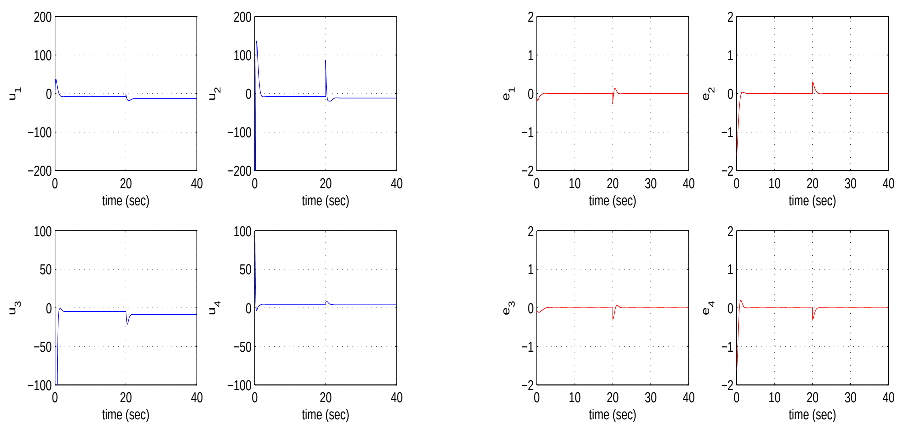

(a) **(b)**

Figure 14: Tracking of setpoint 6 by the induction motor-drive gas compressor (a) Variations of the control inputs u_1 to u_4, (b) Tracking error of state variables x_1 to x_4

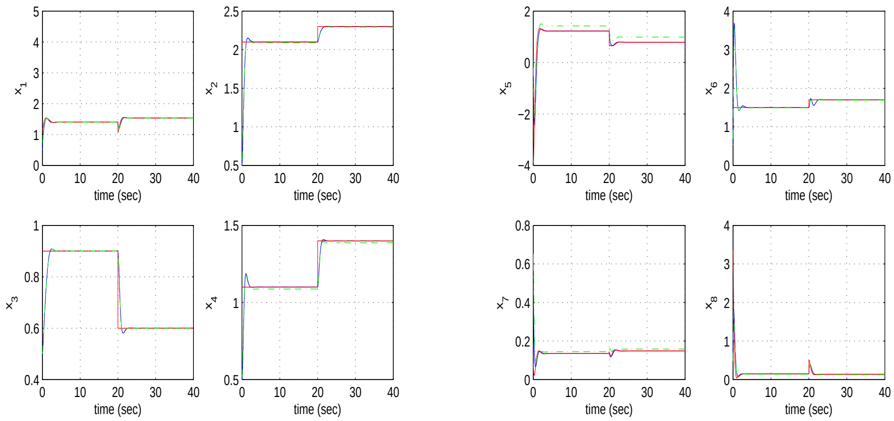

(a) **(b)**

Figure 15: Tracking of setpoint 7 by the induction motor-driven gas compressor (a) Convergence of state variables x_1 to x_4 (blue lines) to the reference setpoints (red lines) and their KF-based estimation (green line), (b) Convergence of state variables x_5 to x_8 (blue lines) to the reference setpoints (red lines) and their KF-based estimation (green line)

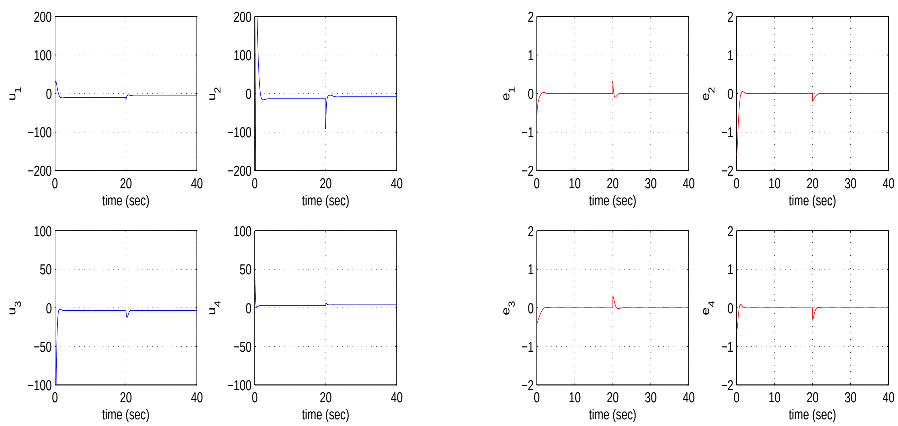

(a) **(b)**

Figure 16: Tracking of setpoint 7 by the induction motor-drive gas compressor (a) Variations of the control inputs u_1 to u_4, (b) Tracking error of state variables x_1 to x_4

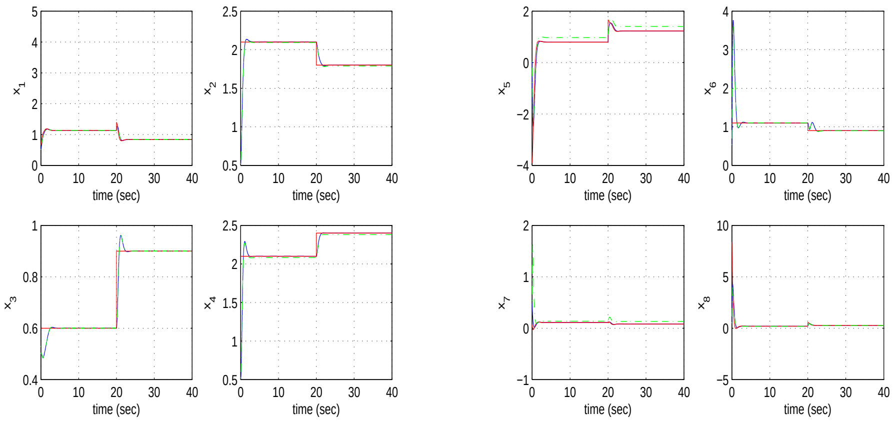

(a) **(b)**

Figure 17: Tracking of setpoint 8 by the induction motor-driven gas compressor (a) Convergence of state variables x_1 to x_4 (blue lines) to the reference setpoints (red lines) and their KF-based estimation (green line), (b) Convergence of state variables x_5 to x_8 (blue lines) to the reference setpoints (red lines) and their KF-based estimation (green line)

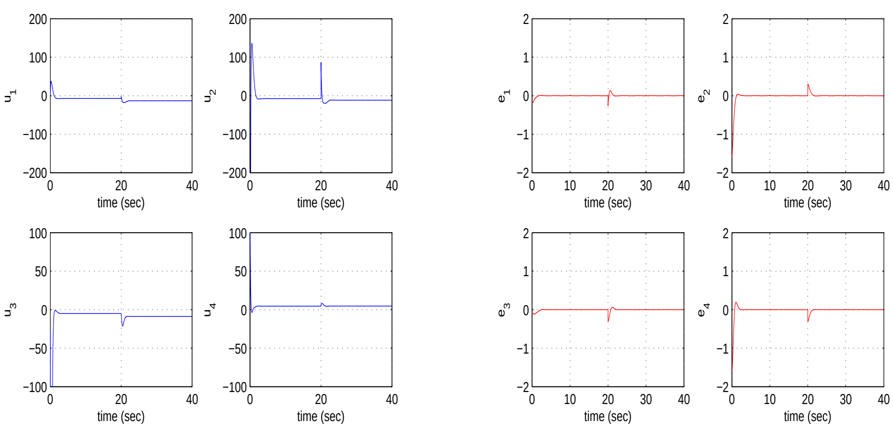

(a) **(b)**

Figure 18: Tracking of setpoint 8 by the induction motor-drive gas compressor (a) Variations of the control inputs u_1 to u_4, (b) Tracking error of state variables x_1 to x_4

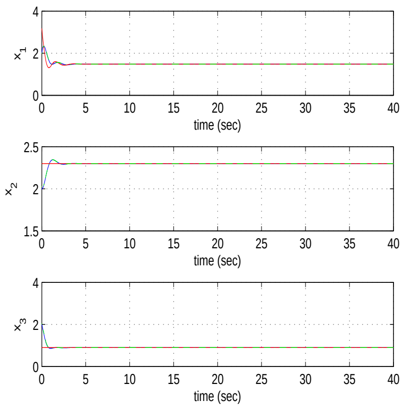

(a)

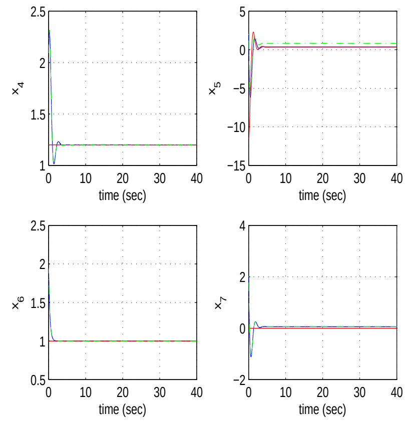

(b)

Figure 19: Tracking of setpoint 1 by the PM synchronous motor-driven gas compressor (a) Convergence of state variables x_1 to x_3 (blue lines) to the reference setpoints (red lines) and their KF-based estimation (green line), (b) Convergence of state variables x_4 to x_7 (blue lines) to the reference setpoints (red lines) and their KF-based estimation (green line)

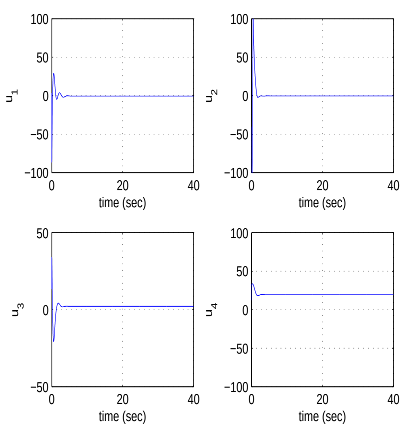

(a)

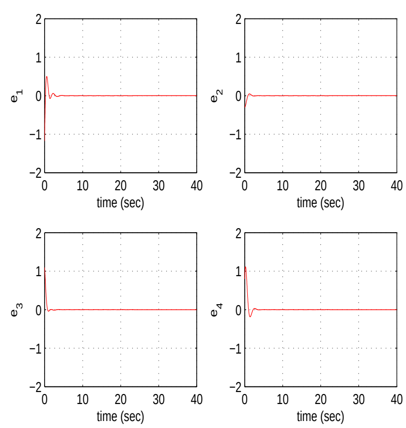

(b)

Figure 20: Tracking of setpoint 1 by the PM synchronous motor-drive gas compressor (a) Variations of the control inputs u_1 to u_4, (b) Tracking error of state variables x_1 to x_4

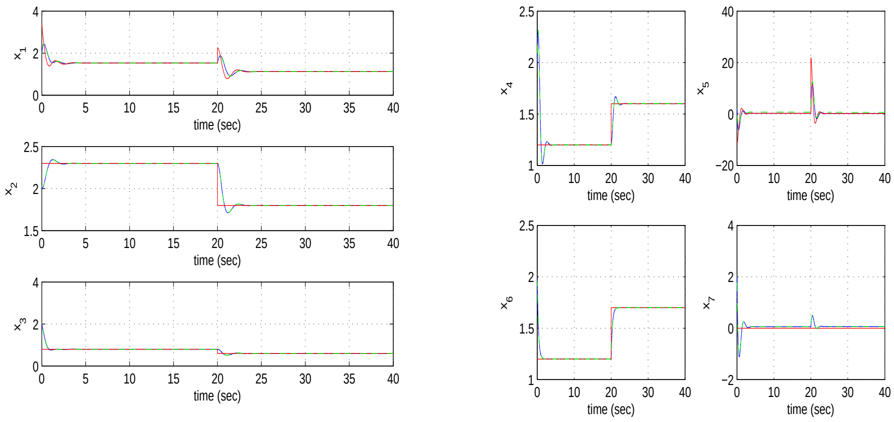

(a) **(b)**

Figure 21: Tracking of setpoint 2 by the PM synchronous motor-driven gas compressor (a) Convergence of state variables x_1 to x_3 (blue lines) to the reference setpoints (red lines) and their KF-based estimation (green line), (b) Convergence of state variables x_4 to x_7 (blue lines) to the reference setpoints (red lines) and their KF-based estimation (green line)

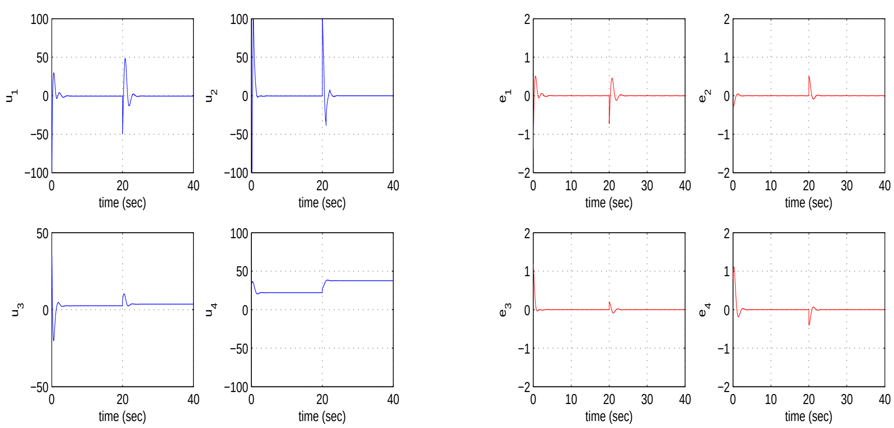

(a) **(b)**

Figure 22: Tracking of setpoint 2 by the PM synchronous motor-drive gas compressor (a) Variations of the control inputs u_1 to u_4, (b) Tracking error of state variables x_1 to x_4

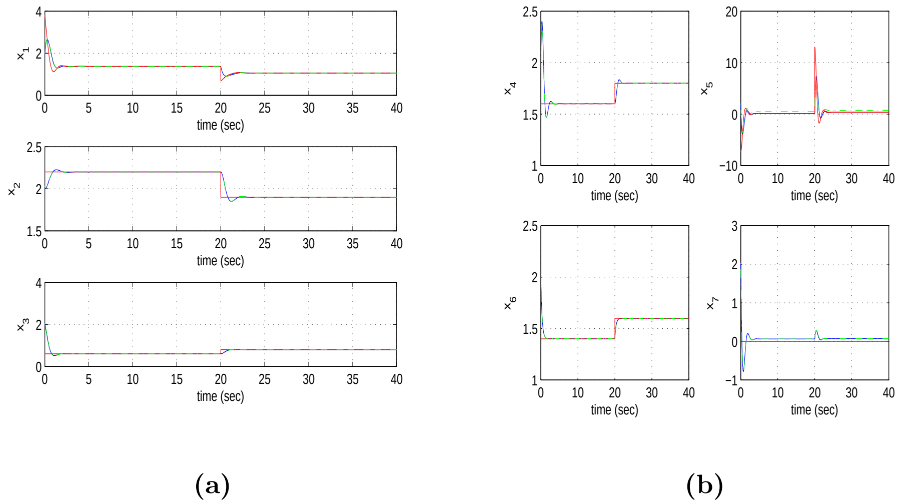

Figure 23: Tracking of setpoint 3 by the PM synchronous motor-driven gas compressor (a) Convergence of state variables x_1 to x_3 (blue lines) to the reference setpoints (red lines) and their KF-based estimation (green line), (b) Convergence of state variables x_4 to x_7 (blue lines) to the reference setpoints (red lines) and their KF-based estimation (green line)

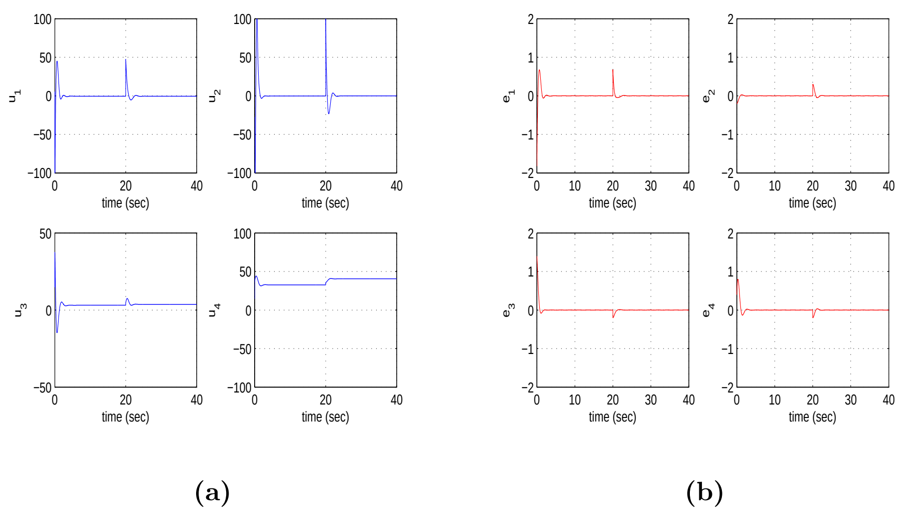

Figure 24: Tracking of setpoint 3 by the PM synchronous motor-drive gas compressor (a) Variations of the control inputs u_1 to u_4, (b) Tracking error of state variables x_1 to x_4

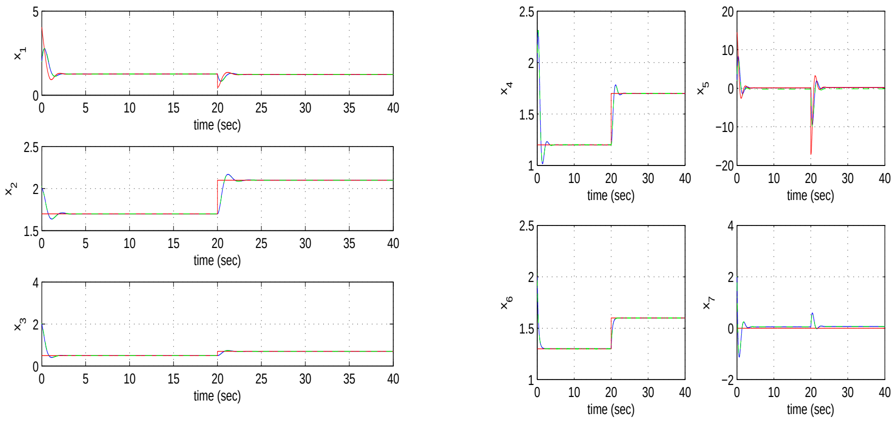

(a) **(b)**

Figure 25: Tracking of setpoint 4 by the PM synchronous motor-driven gas compressor (a) Convergence of state variables x_1 to x_3 (blue lines) to the reference setpoints (red lines) and their KF-based estimation (green line), (b) Convergence of state variables x_4 to x_7 (blue lines) to the reference setpoints (red lines) and their KF-based estimation (green line)

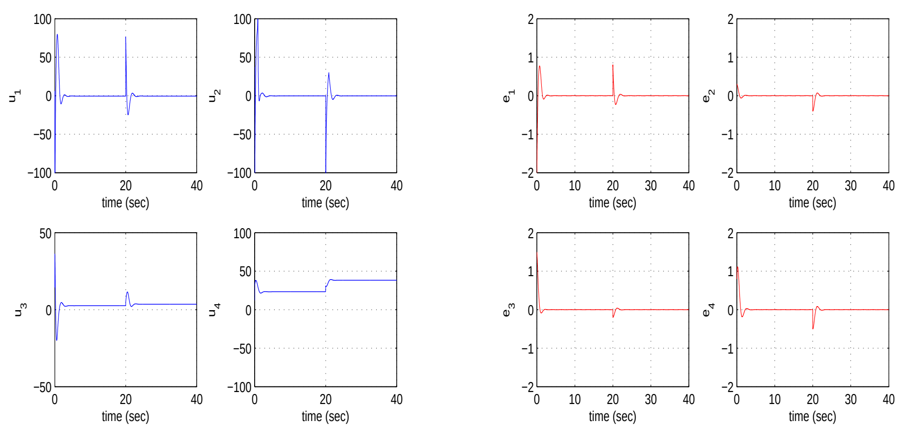

(a) **(b)**

Figure 26: Tracking of setpoint 4 by the PM synchronous motor-drive gas compressor (a) Variations of the control inputs u_1 to u_4, (b) Tracking error of state variables x_1 to x_4

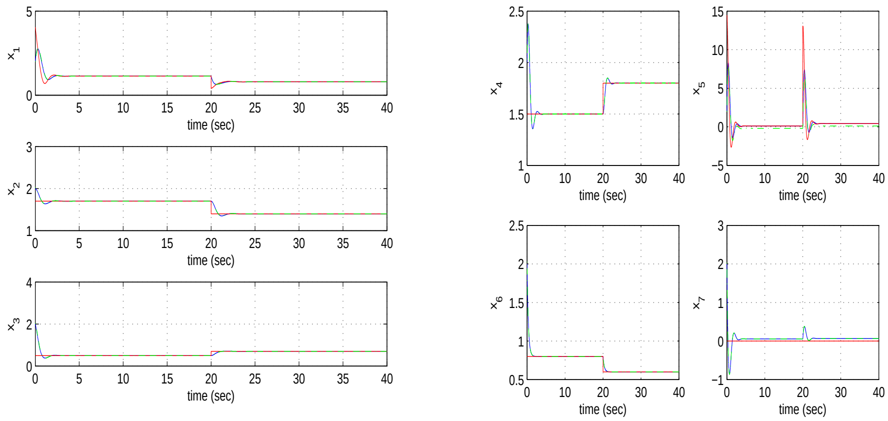

(a) **(b)**

Figure 27: Tracking of setpoint 5 by the PM synchronous motor-driven gas compressor (a) Convergence of state variables x_1 to x_3 (blue lines) to the reference setpoints (red lines) and their KF-based estimation (green line), (b) Convergence of state variables x_4 to x_7 (blue lines) to the reference setpoints (red lines) and their KF-based estimation (green line)

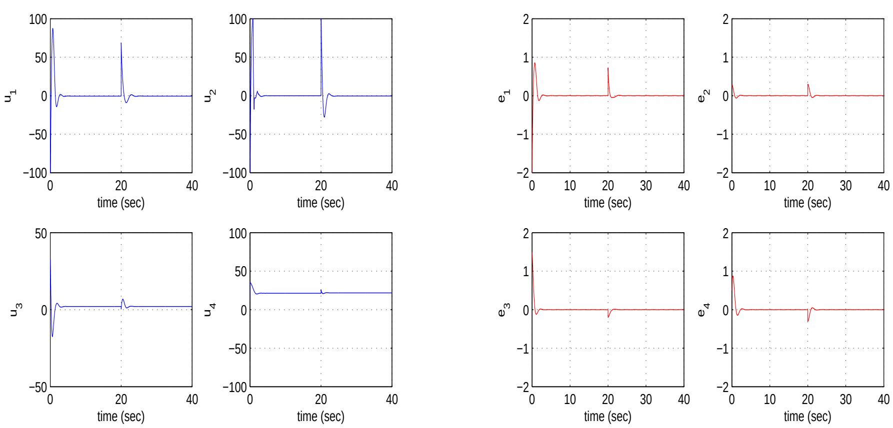

(a) **(b)**

Figure 28: Tracking of setpoint 5 by the PM synchronous motor-drive gas compressor (a) Variations of the control inputs u_1 to u_4, (b) Tracking error of state variables x_1 to x_4

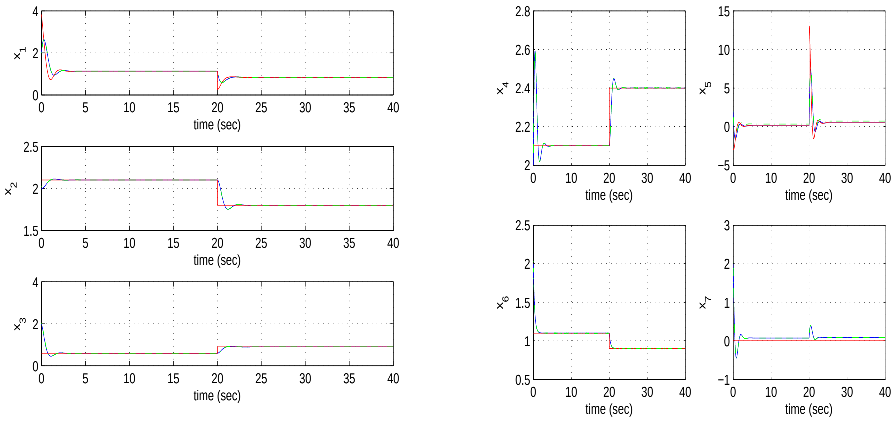

(a) **(b)**

Figure 29: Tracking of setpoint 6 by the PM synchronous motor-driven gas compressor (a) Convergence of state variables x_1 to x_3 (blue lines) to the reference setpoints (red lines) and their KF-based estimation (green line), (b) Convergence of state variables x_4 to x_7 (blue lines) to the reference setpoints (red lines) and their KF-based estimation (green line)

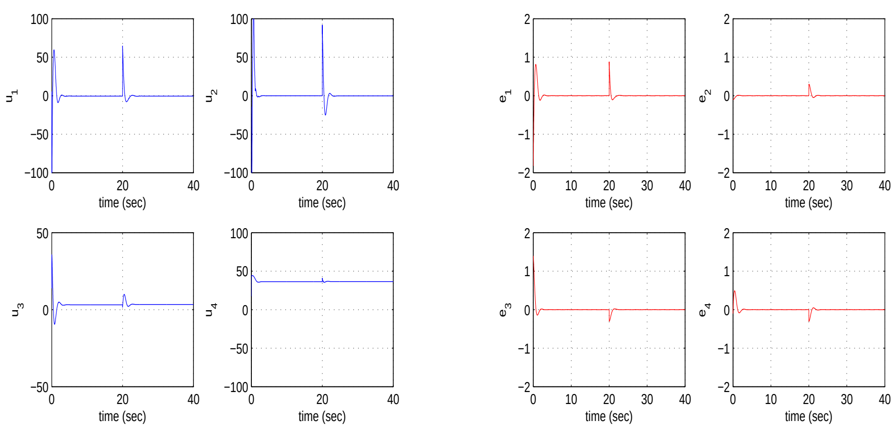

(a) **(b)**

Figure 30: Tracking of setpoint 6 by the PM synchronous motor-drive gas compressor (a) Variations of the control inputs u_1 to u_4, (b) Tracking error of state variables x_1 to x_4

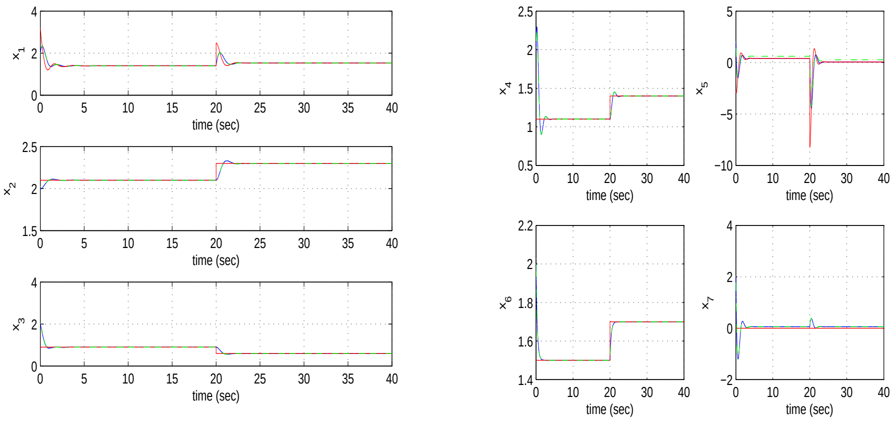

(a) **(b)**

Figure 31: Tracking of setpoint 7 by the PM synchronous motor-driven gas compressor (a) Convergence of state variables x_1 to x_3 (blue lines) to the reference setpoints (red lines) and their KF-based estimation (green line), (b) Convergence of state variables x_4 to x_7 (blue lines) to the reference setpoints (red lines) and their KF-based estimation (green line)

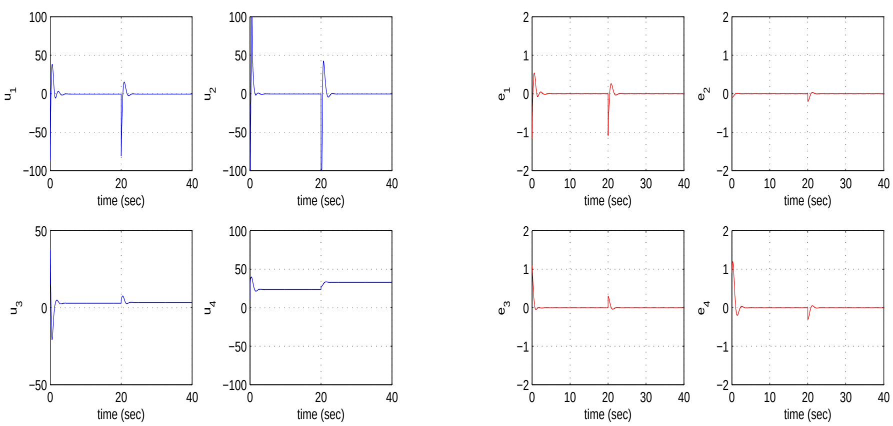

(a) **(b)**

Figure 32: Tracking of setpoint 7 by the PM synchronous motor-drive gas compressor (a) Variations of the control inputs u_1 to u_4, (b) Tracking error of state variables x_1 to x_4

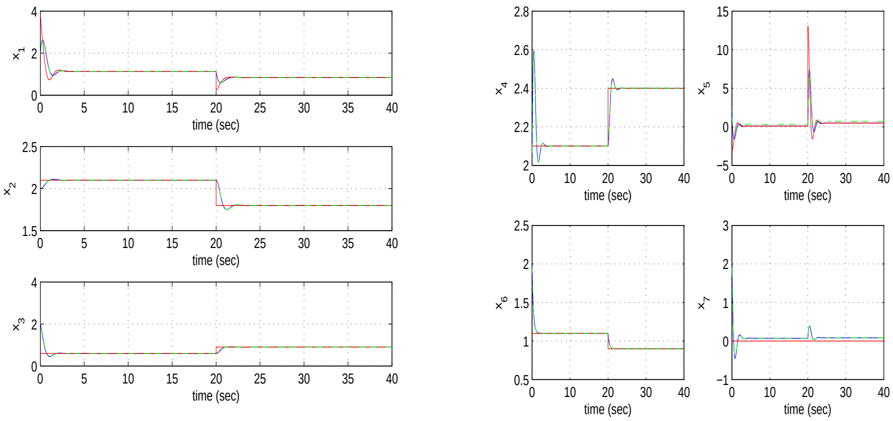

(a) **(b)**

Figure 33: Tracking of setpoint 8 by the PM synchronous motor-driven gas compressor (a) Convergence of state variables x_1 to x_3 (blue lines) to the reference setpoints (red lines) and their KF-based estimation (green line), (b) Convergence of state variables x_4 to x_7 (blue lines) to the reference setpoints (red lines) and their KF-based estimation (green line)

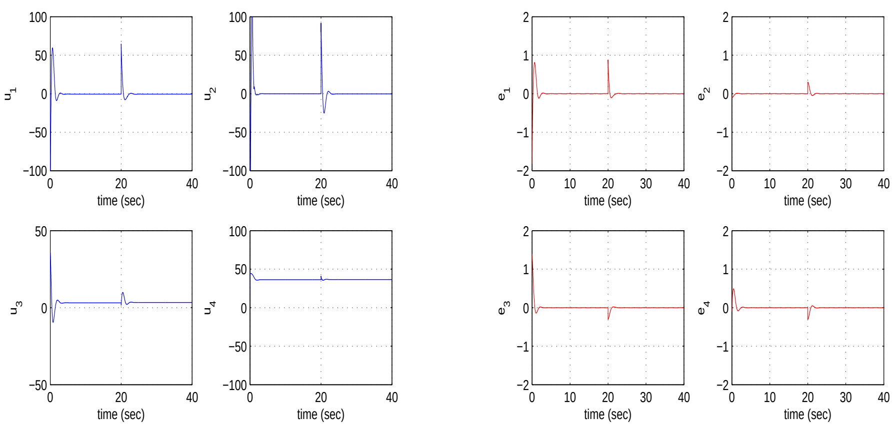

(a) **(b)**

Figure 34: Tracking of setpoint 8 by the PM synchronous motor-drive gas compressor (a) Variations of the control inputs u_1 to u_4, (b) Tracking error of state variables x_1 to x_4

7 Conclusions

The article has proposed a flatness-based control method implemented in successive loops for the dynamic model of IM-driven and PMSM-driven gas compressors. In common approaches to flatness-based control, nonlinear systems undergo a change of state variables and through successive differentiations of their flat outputs one arrives at describing their dynamics in the input-output linearized form and subsequently in the linear canonical (Brunovsky) form. On the contrary, in the proposed flatness-based control method implemented in successive loops there is no need for changes of state variables or forth and back state-space model transformations, and consequently it does not come against singularity cases. The proposed control method achieves fast tracking of reference setpoints. The global stability of the flatness-based control method in successive loops is proven analytically by showing the asymptotic elimination of the tracking error of each one of the subsystems that constitute the integrated system's dynamics. A global stability proof can be also obtained using also Lyapunov analysis. Two case studies have been considered: (i) flatness-based control in successive loops for the dynamic model of a gas-compressor that is actuated by an induction motor, (ii) flatness-based control in successive loops for the dynamic model of a gas compressor that is actuated by a permanent magnet synchronous motor.

In the proposed flatness-based control method implemented in successive loops. the initial nonlinear state-space model of the system is transformed into a chain of subsystems, where for each one of them it is shown that differential flatness properties hold. The state vector of the (i-th) subsystem becomes also a flat outputs vector about it while the state vector of the (i+1)-th subsystem forms a virtual control inputs vector for the i-th subsystem. The proof of differential flatness properties for each one of these subsystems signifies that each one of them can be written in the input-output linearized form and that a stabilizing feedback controller can be designed for each one of them by inverting its dynamics. In this concept, the virtual control inputs vector that stabilizes the (i-th) subsystem should be also a setpoints vector for the (i+1)-th subsystem. Finally, the N-th (last) subsystem in this chain of state-space model contains the real control inputs. The inversion of its dynamics gives the stabilizing feedback controller for the initial nonlinear state-space model. This control signal which achieves stabilization for the initial extended nonlinear state-space model uses recursively the virtual control inputs of the preceding $N-1$ subsystems, by tracing these subsystems backwards that is from the (N-1)-th subsystem to the 1st one. The fine performance of the flatness-based control method in successive loops for IM-actuated and PMSM-actuated gas compressors has been further confirmed through simulation experiments.

Acknowledgements: (a) Gerasimos Rigatos has been partially supported by Grant Ref. 301022 "Nonlinear optimal and flatness-based control methods for complex dynamical systems" of the Unit of Industrial Automation, Industrial Systems Institute, Greece (b) Pierluigi Siano and Mohammed AL-Numay acknowledge financial support from the Distinguished Scientist Fellowship Program, King Saud University, Riyadh, Saudi Arabia.

Data availability statement: Experimental data and software code of the manuscript can be demonstrated upon reasonable request.

References

[1] G. Rigatos, Nonlinear control and filtering using differential flatnesss theory approaches: Applications to electromechanical systems, Springer, 2016

[2] G. Rigatos, M. Abbaszadeh, P. Siano, Control and estimation of dynamical nonlinear and partial differential equation systems: Theory and Applications, IET Publications, 2022

[3] G. Rigatos, Intelligent Renewable Energy Systems: Modelling and Control, Springer, 2016.

[4] G. Rigatos and K. Busawon, Robotic manipulators and vehicles: Control, estimation and filtering, Springer, 2018

[5] G. Rigatos and E. Karapanou, Advances in applied nonlinear optimal control, Cambridge Scholars Publishing, 2020.

[6] S. Bououden, D. Boutat, G. Zheng, J.P. Barbot and F. Kratz, A triangular canonical form for a class of 0-flat nonlinear systems, International Journal of Control, Taylor and Francis, vol. 84, no. 2, pp. 261-269, 2011.

[7] L. Menhour, B. d'Andre'a-Novel, M. Fliess and H. Mounier, Coupled nonlinear vehicle control: Flatness-based setting with algebraic estimation techniques, Control Engineering Practice, Elsevier, vol. 22, pp. 135–146, 2014

[8] F. Nicolau, W. Respondek and J.P. Barbot, How to minimally modify a dynamical system when constructing flat inputs, Internattional Journal of Robust and Nonlinear Control, J. Wiley, 2022.

[9] C. Letelier nd J.P. Barbot, Optimal flatness placement of sensors and actuators for controlling chaotic systemsm Chaos, AIP Publications, vol. 31, no. 10, article No 103114, 2021.

[10] J.Levine, Analysis and Control of Nonlinear Systems: A flatness-based approach, Springer 2009.

[11] S. Riachy, M. Fliess, C. Join and J.P. Barbot. Vers une simplification de la commande non linéaire : l'exemple d'un avion à décollage vertical. Sixième Conférence Internationale Francophone d'Automatique, CIFA 2010, Jun 2010, Nancy, France

[12] M. Fliess and H. Mounier, Tracking control and π-freeness of infinite dimensional linear systems, In: G. Picci and D.S. Gilliam Eds.,Dynamical Systems, Control, Coding and Computer Vision, vol. 258, pp. 41-68, *Birkhaüser*, 1999.

[13] J. Villagra, B. d'Andrea-Novel, H. Mounier and M. Pengov, Flatness-based vehicle steering control strategy with SDRE feedback gains tuned via a sensitivity approach, IEEE Transactions on Control Systems Technology, vol. 15, pp. 554- 565, 2007.

[14] H. Sira-Ramirez and S. Agrawal, Differentially Flat Systems, Marcel Dekker, New York, 2004.

[15] J. Lévine, On necessary and sufficient conditions for differential flatness, Applicable Algebra in Engineering, Communications and Computing, Springer, vol. 22, no. 1, pp. 47-90, 2011.

[16] F. Nicolau, W. Respondek and J.P. Barbot, Construction of flat inputs for mechanical systems, 7th IFAC Workshop on Lagrangian and Hamiltonian methods for nonlinear control, Berlin, Germany, OCt. 2021

[17] J.O. Limaverde Filho, E.C.R. Fortaleza and M.C.M. Campos, A derivative-free nonlinear Kalman Filtering approach using flat inputs, International Journal of Control, Taylor and Francis 2021.

[18] J.P. Barbot, M. Fliess and T. Floquet, An algebraic framework for the design of nonlinear observers with uknown inputs, IEEE CDC 2007, IEEE 46th Intl. Conference on Decision and Control, New Orleans, USA, Dec. 2007

[19] H. Khalil, Nonlinear Systems, Prentice Hall, 1996

[20] G.G. Rigatos and S.G. Tzafestas, Extended Kalman Filtering for Fuzzy Modelling and Multi-Sensor Fusion, Mathematical and Computer Modelling of Dynamical Systems, Taylor & Francis), vol. 13, pp. 251-266, 2007.

[21] M. Basseville and I. Nikiforov, Detection of abrupt changes: Theory and Applications, *Prentice-Hall*, 1993.

[22] G. Rigatos and Q. Zhang, Fuzzy model validation using the local statistical approach, Fuzzy Sets and Systems, Elsevier, vol. 60, no. 7, pp. 882-904,2009.

[23] G. Rigatos, P. Siano and N. Zervos, A new concept of flatness-based control of nonlinear dynamical systems, IEEE INDIN 2015, 13th IEEE Intl. Conf. on Industrial Informatics, Cambridge, UK, July 2015

[24] G. Rigatos, P. Siano, S Ademi and P. Wira, Flatness-based control of DC-DC converters implemented in successive loops, Electric Power Components and Systems, Taylor and Francis, vol. 46, no. 6, pp. 673-687, 2018.

[25] G. Rigatos, Flatness-based embedded control in successive loops for spark ignited engines, Journal of Physics, IOP Publications, Conference Series No 659, 012019, IFAC ACD 2015, Proc. of the 12th European Workshop on Advanced Control and Diagnosis.

[26] G. Rigatos and A. Melkikh, Flatness-based control in successive loops for stabilization of heart's electrical activity, In Proc. ICNAAM 2016, AIP Conf. Proceedings No 1790 060004, Intl. Conf. on Numerical Analysis and Applied Mathematics, 2016

[27] G. Rigatos, P. Wira, M. Abbaszadeh and J. Pomares, Flatness-based control in successive loops for industrial and mobile robots, IEEE IECON 2022, IEEE 48th Annual Conference of the Industrial Electronics Society, Brussels, Belgium, Oct. 2022

[28] G. Rigatos, P. Wira, M. Abbaszadeh and P. Siano, A nonlinear optimal control approach for the Lotka-Volterra dynamical system, IEEE IECON 2022, IEEE 48th Annual Conference of the Industrial Electronics Society, Brussels, Belgium, Oct. 2022

[29] G. Rigatos and P. Siano, Flatness-based control in successive loops for Business Cycles of Finance Agents, Journal of Intelligent Industrial Systems, Springer, vol. 3, pp. 77-89, 2017

[30] X. Han, C. Liu, B. Chen and S. Zhang, Surge disturbance suppression of AMB-rotor systems in magnetically suspended centrifugal compressors, IEEE Transactions on Control Systems Technology, 2022

[31] X. Ma, S. Zhang and K. Wang, Active surge control for magnetically suspended centrifugal compresors using a variable equilibrium point apporach, IEEE Transactions on Industrial Electronics, vol. 66, no. 12, pp. 9363-9393, 2019

[32] G. Torrissi, S. Grammatico, A. CortinovisM. Mercangoz, M. Morari and R.S. Smith, Model predictive approaches for active surge control in centrifugal compressors, IEEE Transactions on Control Systems Technology, vol. 29, no 6, pp. 1947-1960, 2019

[33] T.T. Kristoffersen and C. Holden, Modeling and control of a wet-gas centrifugal compressor, IEEE Transactions on Control Systems Technology, vol. 29, mo. 3, pp. 1175-1190, 2021

[34] Y. Zhou, X. Xiu, M. Qadrdan and J. Wu, Optimal operation of compressor units in gas networks to provided flexibility to power systems, Applied Energy, Elsevier, vol. 290, pp. 116740-116750, 2022

[35] D. Fontaine, S. Liao, J. Padueiro and P.V. Kokotovic, Nonlineear control experiments on axial flow compressor, IEEE Transactions on Control Systems Technology, vol. 12, no. 5, pp. 683-693, 2004

[36] L. Durantay and P. Laboube, Technology trends for LNG compression using innovative electric solutions, IOP Conference Series on Material Sciences and Engineering, vol. 643, no 012149, pp. 118, 2019

[37] Q. Chen, L. Zuo, C. Wu, Y. Li, K. Huo, M. Mehrtush and Y. Cao, Optimization of compressor standby schemes for gas transmission pipeline systems baaed on gas delivery reliability, Reliability Engineering and System Safety, Elsevier, vol. 221, pp. 108351-108363, 2022.

[38] P. Damschke, O. Kahl and J. Lang, Fast and reliable transient simulation and continuous optimization of large-scale gas-networks, Mathematical Methods of Operations Research, Springer, vol. 95, pp. 475-501, 2022

[39] B.K. Kanth Hari, K. Sundar, S. Srinivashan, A. Zlotnik and R. Bent, Operation of natural gas pipeline networks with storage under transient flow conditions, IEEE Transactions on Control Systems Technology, vol. 30, no. 2, pp. 667-679, 2022.

[40] V. Dvornik, D. Mallapragada, A. Batterud, J. Kazempour and P. Pinson, Electric Power Systems Research, Elsevier, vol. 212, pp. 108388-108394, 2022.

[41] R.L. Meira, M.A.F. Martins, R.A. Kalid and G.M.N. Costa, Implementable MPC-based surge avoidance nonlinear control strategies for non-ideally modelled natural gas compression systems, Journal of Natural Gas Science and Engineering, vol. 102, pp. 104573-104586, 2022.

[42] R.S. Gesser, R. Sartori, T.P. Damo, C.M. Vettorazzo, L.B. Becker, D.M. Lima, M.L. de Lima, L.D. Ribeiro, M.C. M.C. Campos and J.E. Namey Rico, Advanced control appliied to a gas compression system of an offshore platform: From modelling to related system infrastructure, Journal of Petroleum Science and Engineering, vol. 208, pp. 109428-109447, 2022

[43] S.A.C. Girardo, R.C. Supelano, T.C. d' Avila, B.D.O Capron, L.D. Ribeiro, M.M. Campos and A.R. Secchi, Model-predictive control with dead-time compensation applied to a gas-compression system, Journal of Petroleum Science and Engineering, Elsevier, vol. 203, pp. 108580-108588, 2021

[44] B. Behegen and T,M. Gravdahl, Active surge control of compression system uising drive torque, Automatica, Elsevier, vol. 44, pp. 1135-1140, 2008

[45] G. Torrisi, V Jaramillo, J.R. Ottewill, M. Mariethoz, M. Morari and R.S. Smith, Active surge control of electrically driven cntrifugal compressors, 2015 European Control Conference, Linz, Austria, July, 2015.

[46] J.T. Gravdahl, O. Egeland and S.O. Vatland. Drive torque actuation in active surge control of centrifugal compressors, Automatica, Elsevier, vol. 38, pp. 1881-1893, 2002

[47] K.M. Arthur, M. Basu and S.Y. Yoon, Stabilization of compressor surge : systems with uncertain equilibrium flow, ISA Transactions, Elsevier, vol. 93, pp. 115-134, 2019

[48] T.W. Chen, J.R. Ahn, H.H. Lee, H.G. Kim and E.C Nho, A novel strategy of efficiency control for a linear compressor system driven by a PWM inverter, IEEE Transactions on Industrial Electronics, vol. 55, no. 1, pp. 296-30, 2008

[49] N.A. Chaturvedi and S.P. Bhat, Output feedback semiglobal stabilization of stall dynamics for preventing hysteresis and surge in axial-flow compressors, IEEE Transactions on Control Systems Technology, vol. 14, no. 2, pp. 301-307, 2006

[50] T. Bentaleb, A. Cacitti, S. De Franciscis and A. Garulli, Model Predictive Control for Pressure Regulation and Surge Prevention in Centrifugal Compressors, IEEE ECC 2015 Linz, Austria, July 2015

[51] J. Hang, W.J. Lee, S. Park, Y. Kim, K.J. Lee and C. Han, Improved control strategy for fixed-speed compressors in parallel system, Journal of Process Control, Elsevier, vol. 53, pp. 57-69, 2017.

[52] K. Jones, A. Cortinovis, M. Mercengoz and H.J. Ferreau, Distributed Model Predictive Control of centrifugal compressor systems, 20th IFAC World Congress, Toulouse, France, July, 2017.

[53] C. Xie and H. Imani Marrani, Design of a robust LMI-based model predictive control method for surge instability in interconnected compressor systems, Systems Science and Control Engineering, vol. 9, no. 1, pp. 358-368, 2021.

[54] P. Miloslavljevic, A. Cortinovis, R. Schneider, T. Faulwasser, M. Mercangoz and D. Bonvin, Optimal load sharing for serial compressors with modifier adaptation, IEEE ECC 2018, European Control Conference 2018, Limassol, Cyprus, June 2018.

[55] H. Imani, M.R. Jahed-Matlagh, K. Salashoor, A. Ramezani and A. Moarefianpur, Robust decentralized model predictive control approach or a multi-compressor system surge instability including piping acoustic, Cogent Engineering, Taylor and Francis, vol. 5, no. 1, pp. 148381, 2018.

[56] A. Cortinovis, D. Pareschi, M. Mercangoz and T. Besselmann, Model-predictive anti-surge control of centrifugal compressors and variable speed dries, Proc. 2012 IFAC Workshop on Automatic Control in Offshore Oil and Gas Production, June 2012, Trodheim, Norway

[57] A. Cortinovis, H.J. Ferreau, D. Lewandowski and M. Mercangoz, Safe and efficient operation of centrifugal compression using linearized MPC, 53rd IEEE Conference on Decision and Control, Los Angeles, USA, Dec. 2005

[58] S. Dominic, Y. Lohr, A. Schwung and S.X. Ding, PLC-based real-time realization of flatness-based feed-forward control for industrial compressor systems, IEEE Transactions on Industrial Electronics, vol. 64, no. 2, pp. 1323-1331, 2017

[59] B.H. Bue, S.K. Sul, J.H. Kwon and J.S. Bycon, Implementation of sensorless vector control for super-high-speed PMSM turbo-compressors, IEEE Transactions on Industry Applications, vol. 39, no. 3, pp. 811-818, 2003

[60] C.J. Backl, J.T. Gravdahl and S. Skogestad, Robust control of a two-state Greitzer compressor model by state-feedback linearization, IEEE CCA 2016, IEEE 2016 Conference on Control Applications, Buenos Aires, Argentiaa, Sep. 2016

[61] L. Giarré, D. Bauso, P. Falugi and B. Bamie, LPV model idneitification for gain scheduling control: An application to rotating stall and surge control problem, Control Engineering Practice, Elsevier, vol. 14, pp. 351-361, 2006

[62] N. Tangesdal, T.T. Kristofferesen and C. Holden, Applied nonlinear compressor control with gain scheduling and state estimation, 3rd IFAC Workshop on automatic control in offshore, Oil anf Gas Production, Esbjerg, Denmark, June 2011

[63] X. Fu, L. Fu and H. Nalekizadeh, Finite-time action fuzzy sliding mode approach for deep surge control in nonlinear distorted compressor system with uncertainty in characteristic curve, Automatika, Taylor and Francis, vol. 62, no. 3-4, pp. 530-540, 2021

[64] C. Xie and M.T. Marrani, Design of a ribust LMI-based model predictive control method for surge instability in interconnected compressor systems in the presence of uncertianty and disturbance, Systems Science and Control Engineering, Taylor and Francis, vol. 9, no. 1, pp. 358-368, 2021

[65] L. Fu, X. Fu, M.T. Ziabari, Finite-time adaptive sliding-mode control for compresor surge with uncertain characteristics in the presence of disturbances, Systems Science and Control Engineering, Taylor and Frncis, vol. 9, no. 1, pp. 369-379, 2021.

[66] K.O. Bainov, E.A. Lomonova, A.J.A. Vandenput and A. Tyagunov, Surge control of the electrically driven centrifugal compressors, IEEE Transactions on Industry Applications, vol. 42, no. 6, pp. 1523-1532, 2006

[67] B. Blunier, M, Pucci, G. Cirrincione and A. Miraoui, A stroll compressor with a high-performance induction motor drive for the air management of a PEMFC sysstem for automotive applications, IEEE Transactions on Industry Applications, vol. 44, no. 6, pp. 1966-1976, 2008

[68] A. Cotrinovis, M. Mercengoz, T. Besselmann, A.M. Ditlefsen, To.O. Stuva, S. Van de Moorted and E.Lunde, Enabling voltage drop ride-throughs of large electric driven gas compressors, Journal of Process Control, Elsevier, vol. 74, pp. 76-87, 2019

[69] Y. Notohara, D. Li, Y. Iwagi, M. Tomura and K. Tsukei, Study on vibration suppression control for rorary compressors, IEEJ Journal on Industry Applications, vol. 10, no. 4, pp. 481-486, 2021.

[70] N. Uzhegov, A. Smirnov, C.H. Park, J.H. Ahn, J. Heikinnen and J. Pyrhonnen, Design aspects of high-speed electrical machines with active magnetic bearings for compressor applications, IEEE Transactions on Industrial Electronics, vol. 64, no. 11, pp. 8427-8436, 2019.

[71] B.H. Bue, S.K. Sul, J.H. Kwon and J.S. Bycon, Implementation of sensorless vector control for superhigh- speed PMSM turbo-compressors, IEEE Transactions on Industry Applications, vol. 39, no. 3, pp. 811-818, 2003

[72] E. Liu, L. Lv, Y.Yi and P. Xie, Research on the steady operation optimization model of natural gas pipeline considering the combined operation of air coolers and compressors, IEEE Access, vol 7, pp. 83521-83535, 2019

[73] S. Budini and N.F. Thornhill, Control of centrifugal compression via model predictive control for enhanced oil recovery applications, 2nd IFAC Workshop on Automatic Control in Offshore Oil and Gas Production, Florianapolis, Brazil, May 2015

[74] M.T. Ziabari, M.R. Jahed-Motlagh, K. Salashoor, A. Ramazani and A. Mourefianpur, Robust adaptive control of surge instability in constant speed centrifugal compressors using tube-MPC, Cogent Engineering, Taylor and Francis, vol. 4, no. 1, pp. 1-21, 2017

[75] F. Jeng Lin, S.Y. Lee, H.C. Chsang and Z.Y. Kuo, Design and implementation of sensorless DC inverter-fed compressor drive system, Journal of the Chinese Institute of Engineers, Taylor and Francis, vol. 35, no. 6, pp. 655-673, 2012

[76] M. Zagorowska, C Skourup and N.T. Thornhill, Influence of compressor degradation on optimal operation of a compressor system, Computers and chemical engineerinng, Elevier, vol. 143, pp. 107104, 2020.

[77] P. Milosavljevic, R. Schneider, A. Cortinovis, T. Faulwasser and D. Bonvin, A distributed feasible-side convergent modifier adaptation scheme for interconnected systems with application to gas compressor station, Computers and Chemical Engineering, Elevier, vol. 115, pp. 474-486, 2018.

[78] P. Milosavljevic, A. Cortinovis, A.G. Marchetti, T. Faulwasser, M. Mercangoz and D. Bonvin, Optimal load sharing of parallel compressor via modifier adaptation, IEEE CCA 2016, IEEE 2016 Conference on Control Applications, Buenos Aires, Argentina, Sep. 2016.

[79] S. Kumar and A. Cortinovis, Load sharing optimization for parallel and serial compressor systems, IEEE CCTA 2018, IEEE 2018 Conf. on Control Technology and Applications, Hawai, USA, Aug. 2017.

[80] X. Li, T. Cui, K. Huan and X. Ma, Optimization of load sharing for parallel compressors using a novel hybrid intelligent algorithm, Energy Science and Engineering, J. Wiley, vol. 9, pp. 330-342, 2021.

[81] P. Milosavljevic, A.G. Marchetti, A. Cortinovis, T. Faulwasser, M. Mercangoz and D. Bonvin, Real-time optimization for load sharing for gas compressors in the presence of uncertainty, Applied Energy, Elsevier, vol. 272, pp. 114853, 2020.

[82] M. Zagorowska, N. Thornhill, T. Haugen and Skourup, Load sharing strategy taking account of compressor degradation, IEEE CCTA 2018, IEEE 2018 Conference on Control Technology and Applications, Copenhagen, Denmark, Aug. 2018.

[83] M. Zagorowska and N.F. Thornhill, Optimal operation of compressors in terms of power and efficiency, IEEE 2021 Mediterranean Conf. on Control and Automation, June 2021, Bari, Italy.

[84] J Jung, W.J. Lee, S. Park, Y. Kim, C.J. Lee, and C. Han, Improved control strategy for fixed-speed compressors in parallel system, Journal of Process Control, Elsevier, vol. 53, pp. 57-69, 2017

[85] M. Peyrl and A. Cortinovis, Computationally efficient solution of a compressor load sharing problem using the alternating direction method of multiplies, IEEE ECC 2015, European Control Conference 2015, Linz, Austria, July 2015

[86] P. Milosavljevic, R. Schneider, A. Cortinovis, T. Faulwasser and D. Bonvins, A distributed feasible-side convergent modifier-adaptation scheme for interconnected systems, with application to gas-compressor stations, Computers and Chemical Engineering, Elsevier, vol. 115, pp. 474-486, 2018

[87] Z. Hao, Y. Yang, Y. Tian, Y. Gang, C. Zhang, H. Song, Z. Hao and J. Zhang, Phase-lead compensation of a [hase-locked loop in an IPMSMfor air conditioner compressors, IEEE Transactions on Energy Conversion, vol. 35, no. 2, pp. 1090-1100, 2021.

[88] Z. Zhu, J. Deng, H. Ouyama and X. Dou, Optimized sampling mechanism for full-state current control of LCL-equipped high-speed PMSM for fuel-cell air compressor, IEEE Transactions on Transportation Electrification, pp. 1-12, 2023.

[89] J. Hu, N. Zhou, R. Guo, G. Wang, G. Zhang and D. Xu, Torque ripple compensation with anti-over-voltage for electrolytic capacitorless PMSM compression drives, IEEE Journal on Emerging and Selected Topics in Power Electronics, vol. 10, no. 5, pp. 6148-6159, 2022.

[90] C.S. Park, J.H. Kim, S.H. Park, Y.D. Yoon and M.S. Lim, Multi-physics characteristics of PMSM for compressor according to driving mode considering PWM frequency, IEEE Access, vol. 10, pp. 114490-1114500, 2022.

[91] G. Rigatos, M. Abbaszadeh, B. Sari, P. Siano, G. Cuccurullo and F. Zouari, Nonlinear optimal control for a gas compressor driven by an induction motor, Results in Control and Optimization, Elsevier, vol. 11, pp. 1-24, 2023.